The Effect of High-Fat Diet and Exercise on Non-Alcoholic Fatty Liver Disease and Glycemic Control

Abinas Uthayakumar

A THESIS SUBMITTED TO THE FACULTY OF GRADUATE STUDIES IN PARTIAL FULFILMENTS OF THE REQUIREMENTS FOR THE DEGREE OF

MASTER OF SCIENCE

GRADUATE PROGRAM IN KINESIOLOGY AND HEALTH SCIENCE
YORK UNIVERSITY
TORONTO, ONTARIO

AUGUST 2015

Abstract

This study investigates the effects of chronic high-fat diet (HFD) and endurance training on Non-Alcoholic Fatty Liver Disease (NAFLD) and glycemic control. Here we report that chronic HFD promotes hepatic steatosis to an extent, which impairs whole body glucose metabolism. Moreover, we illustrate the effectiveness of exercise in attenuating HFD-induced NAFLD. In addition to NAFLD treatment, exercise improves whole body glycemic control and insulin sensitivity. Measures of gluconeogenic markers indicate a reduction in gluconeogenesis (GNG) to be partially attributable to the improved glucose regulation. Importantly, we present the novel finding that chronic endurance exercise reduces the rate of hepatic glycogen synthesis despite improvements in glycemia. Thus, it appears glucose has alternate metabolic fates in the body which forces mobilization rather than storage of glucose in a trained system. Taken together, it appears exercise is an effective therapeutic tool, which can significantly improve the deleterious effects of chronic HF-feeding.

Acknowledgements

Dr. Rolando Ceddia – Thank you for all the support you've given me over the last two years. The values and skills I've learned from you are priceless. When I first came to you I had never even touched a pipette (or a rat for that matter) and I knew practically nothing about research. At that time you used to compare me to yourself. You said you came into research with nothing and everything you currently know came from the initiatives you took to teach yourself. That alone gave me a boost of confidence (as did many of my talks with you). You always had faith in me, even in times when I doubted myself. I am grateful to have had the opportunity to work in your lab and I couldn't have asked for a better supervisor.

To my Parents – Thank you for all the love and support you've given me. I owe my success entirely to the both of you. The sacrifices you've made to get me this far are endless and I hope I've made you proud. I love you both.

Diane Sepa-Kishi – Kishi! I still can't believe you're half Japanese. I have a lot of respect for your people (I love their cars and sushi). I remember the first day I came in I didn't even see you sitting there until Rolando told me we have a PhD student. From the moment he introduced us you've been nothing but supportive the entire way. To me you are a "mini Rolando". Although I may have poked you during our GTT, I really enjoyed working with you. I've learned a lot from you and I can't wait to come back for your defense so I can call you Dr. Kishi...or is it Dr. Sepa-Kishi?

Michelle Victoria Wu – Wu wing See! You have to read this entire thing in a Chinese accent. I don't know about you but I'll always miss making those accents on a daily basis. To me you're the coolest asian girl in the world because a) you have a bike, and b) you want to be a firefighter! God forbid, if I ever end up in a fire, I hope you're the one to save me. I'm glad that in the process of doing our masters together I've made an amazing friend.

Arta Mohasas – Ceddia ___! You're supposed to say Rabs! What made dissections so much fun was having someone to make accents and sing songs with. I still remember the day we slept over in the lab and the girls were wondering where we were the next morning. One thing I won't forget is when you whistled at some random girl in the hallway and made her think I did it. I still have to get you back for that so sleep with one eye open Mohasas! I hope camp and everything works out well for you.

Navnit Banwait – Thank you for being so supportive throughout the entire way. I know it can get quite annoying hearing about research and what happens in the lab all the time. I hope I can return the favor and be there as you finish your last year before you're officially an OT!

Table of Contents

List of Figures

List of Acronyms

1,3 BPG	1,3-bisphosphoglycerate
2-PG	2-phosphoglycerate
3-PG	3-phosphoglycerate
AC	Adenylate Cyclase
ALT	Alanine transaminase
ATP	Adenosine Triphosphate
AKT/PKB	Protein Kinase B (PKB and AKT are used interchangeably)
AMPK	AMP-activated protein kinase
cAMP	Cyclic adenosine monophosphate
Ex SC	Exercise standard chow
Ex HF	Exercise high fat
F6P	Fructose 6-Phosphate
F6Pase	Fructose6-Phosphatase
FBP	Fructose 1,6-bisphosphate
FBPase	Fructose 1,6-bisphosphatase
FFA	Free fatty acid
G3P	Glyceraldehyde 3-phosphate
G6P	Glucose 6-Phosphate
G6Pase	Glucose 6-Phosphatase
GAPDH	Glyceraldehyde phosphate dehydrogenase
GK	Glucokinase
GLUT2	Glucose transporter 2
GLYK	Glycerol Kinase
GNG	Gluconeogenesis
GP	Glycogen phosphorylase
GPCR	G-Protein coupled receptor
GSK3	Glycogen synthase kinase
GYS	Glycogen synthase
HF	High fat
HFD	High fat diet
IPGTT	Intraperitoneal glucose tolerance test
IPPTT	Intraperitoneal pyruvate tolerance test
IRS	Insulin receptor substrate
LDH	Lactate dehydrogenase
MAS	Malate aspartate shuttle
MDH	Malate dehydrogenase
NAFLD	Non-Alcoholic Fatty Liver Disease
OAA	Oxaloacetate
PC	Pyruvate carboxylase
PDK1	Phosphoinositide-Dependent Kinase-1
PEP	Phosphoenolpyruvate
PEPCK	Phosphoenolpyruvate Carboxykinase
PGAM	Phosphoglycerate mutase
PGC-1α	Peroxisome proliferator-activated receptor (PPAR)-γ co-activator-1α
PGK	Phosphoglycerate kinase

PHI	Phosphohexoisomerase
PIP2	Phosphatidylinositol 4,5-bisphosphate
PIP3	Phosphatidylinositol (3,4,5) Trisphosphate
PI3K	Phosphoinositide 3-kinase
PK	Phosphorylase Kinase
PKA	Protein Kinase A
PKB	Protein Kinase B
PP1	Protein Phosphatase 1
SC	Standard Chow
Sed SC	Sedentary standard chow
Sed HF	Sedentary high-fat
SREBP-1c	Sterol Regulatory Element-Binding Protein-1c
STZ	Streptozotocin
TAG	Triglyceride

1. Introduction

The obesity epidemic, which once was a western crisis, has evolved into a global concern. As a result, an alarming number of people are spending more of their lives in a morbidly obese state (1). Fast food chains whose products typically consist of excessive fats and are hyper-caloric in nature are spreading rapidly even in several underdeveloped nations. Moreover, modern societies are heavily built around technology, and focus on automotive transportation while neglecting cyclers, and pedestrians alike (2). As a result, people take this as an invitation to welcome a sedentary lifestyle making it difficult for them to meet the Canadian recommended guidelines for physical activity of 150min/week (3).

In 2008 it was estimated that globally, 1.46 billion adults were overweight in addition to another 502 million obese adults (4). These obesity trends go hand in hand with type 2 diabetes (T2D) and NAFLD. In fact, NAFLD is seen in over 65% of people with T2D and over 90% of morbidly obese patients (5). Patients with NAFLD display excessive hepatic fat accumulation that exceeds 5% of the liver's weight. Due to the lack of signs/symptoms, this liver pathology often goes undetected unless scanned for using ultrasound or diagnosed through liver biopsy (6). Despite being a silent condition, the effects of NAFLD are suffered at both a hepatic and systemic level.

Individuals with NAFLD often display poor glucose and lipid metabolism. This can often further aggravate an already impaired system, as is the case with diabetics. A study by Kelley et al., found that patients who were diabetic but also had fatty liver were significantly more insulin resistant than those with diabetes

alone (7). Moreover, it has been reported that the production of both fat and glucose is elevated in these individuals while removal of these substrates is impaired or insufficient (8–10). Lastly, in its later stages, NAFLD can end in hepatocellular carcinoma and resultant liver failure (11). Therefore, treating this condition in its early stages is critical to prevent further morbidities and possible mortality.

Aside from bariatric surgery, which is limited almost exclusively to patients in the later stages of NAFLD or severe obesity, there are no therapeutic alternatives to treat fatty liver thus far. Therefore, healthcare professionals have turned to dietary interventions in conjunction with regular exercise as the primary means to reduce fat accumulation in the liver. Reducing both dietary fats and overall caloric intake is believed to prevent or in some cases reverse fatty liver. Interestingly, a reduction in ectopic fat accumulation following chronic endurance exercise has been reported in rats fed a high-fat diet (HFD) (12, 13).

Accordingly, this study investigates the effects of chronic high fat feeding and endurance training on NAFLD and glycemic control. We analyze numerous indicators of glucose and lipid metabolism as well as measure intra-hepatic fat content as a means of identifying fatty liver.

2. Literature Review

2.1 Liver

The liver is arguably the most versatile organ in the body. It is crucial for the elimination of toxins, production of bile, and maintenance of blood glucose homeostasis among other roles. It is a highly perfused organ consisting of two blood supplies. Given its close proximity to the intestines, the liver receives nutrient rich blood through the portal vein (75% of blood supply). On the other hand, it receives oxygen-rich blood through the hepatic artery (25% of blood supply). Upon delivering nutrients and oxygen to the liver, blood exits the liver through the hepatic vein and returns to the heart.

Subsequent to an overnight fast, many of the hormones including insulin are at their basal levels (14). During this time, the liver is responsible for maintaining blood glucose levels within a range of 4-7mM despite not having any incoming carbohydrates. It is crucial that this process occurs as organs and cells such as the brain and red blood cells rely almost exclusively on glucose as a fuel substrate. As such, the liver has two primary means of maintaining plasma glucose in a fasted state. First, it may undergo a catabolic process known as glycogenolysis to liberate glucose molecules from glycogen. This accounts for about 75% of the glucose in circulation under basal conditions. Next, the liver is also able to actively produce glucose through non-carbohydrate sources including lactate, alanine, pyruvate and glycerol. The *de novo* synthesis of glucose, which occurs almost exclusively in the liver, is known as gluconeogenesis (GNG) and accounts for the remaining 25% of circulating glucose during prolonged fasting (14).

In a fed state, the liver remains the principal site of glucose disposal while muscle and adipose tissue represent comparatively minor sites. Under these conditions, hepatic plasma insulin concentrations are 3-10 fold higher than in circulation in an attempt to minimize post-prandial elevations in blood glucose (14). This facilitates a number of processes including uptake of glucose into peripheral tissues, the storage of glucose as glycogen, and the suppression of GNG and glycogenolysis. Upon receiving a bolus of glucose, nearly 60% of it are stored within the liver, 15% is used by muscle and adipose tissue in an insulin-dependent manner, while the remaining 25% is used to meet the energy demands of the brain and other tissues where insulin is not necessary for glucose uptake. Interestingly, this 25% is thought of as a glycogen sparing mechanism because the body no longer needs to break down existing glycogen to meet the energy demands of glucose dependent tissues and cells (14).

2.2 Hepatic Glucose Metabolism

2.2.1 Glycogen Synthesis

After a meal, the liver uptakes a large quantity of glucose through its insulin-independent glucose transporter 2 (GLUT2) and promotes the storage of glucose as glycogen. Although it is able to uptake glucose in the absence of insulin, the conversion of glucose to glycogen is partly an insulin-mediated process (15, 16).

Given the importance of the liver in glycemic control, glucose absorbed by the intestines immediately enters the liver through the portal vein. The liver absorbs a large quantity of glucose and any excess glucose exits from the hepatic vein. The hepatic vein merges into the inferior vena cava, which returns to the heart. This blood is re-oxygenated in the lungs, and re-circulated out the aorta. The descending portion of the aorta branches off to supply the oxygenated blood to various organs including the liver (through the hepatic artery) and the pancreas. Upon sensing the concentration of glucose in the blood, the β-cells of the pancreas release insulin. This insulin-rich blood enters hepatic circulation through the portal vein upon which the liver can undertake several insulin-mediated processes including the incorporation of glucose into glycogen.

Once insulin reaches the liver, it binds to the insulin receptor and promotes autophosphorylation of the receptor. As a result, the insulin receptor is able to interact with insulin receptor substrates (IRS), namely IRS-1 and phosphorylate these proteins at multiple tyrosine residues. Phosphorylated IRS-1 interacts with the p85 regulatory subunit of phosphoinositide 3-kinase (P13K) and

recruits the catalytic p110 subunit to the plasma membrane. This serves to phosphorylate phosphatidylinositol 4,5-bisphosphate (PIP2) that is anchored to the lipid bilayer of the cell membrane by two fatty acids. Additional phosphorylation of PIP2 forms phosphatidylinositol (3,4,5) trisphosphate (PIP3), which activates phosphoinositide-dependent kinase-1 (PDK1) and ultimately phosphorylates and activates AKT, also known as Protein Kinase B (PKB). Phosphorylation of AKT at Ser^{473} promotes the subsequent phosphorylation and inactivation of glycogen synthase kinase 3 (GSK3); a protein which otherwise phosphorylates and inhibits glycogen synthase (GYS) activity (17). GSK3 is present in both α and β isoforms and its phosphorylation on an N-terminal regulatory site (namely Ser^{21} and $Seri^{9}$ on α and β, respectively) remove its inhibitory effects on GYS. Insulin simultaneously promotes activity of Protein Phosphatase 1 (PP1). Activated PP1 dephosphorylates the Ser^{641} (Site 3a) residue on the COOH-terminal of GYS in an insulin-dependent manner. Dephosphorylated GYS is active and therefore results in the incorporation of glucose 6-phosphate (G6P) into glycogen (15, 18).

Although glycogen synthesis is in part an insulin-mediated process in the liver, current literature indicates that hepatic glycogen synthesis is largely dependent on substrate availability rather than hormonal influence (19). Hence, activation of GYS is believed to be proportional to blood glucose concentration, while the presence of insulin simply facilitates the process to a smaller extent (19). As a consequence, under normal conditions a large portion of the glucose entering the liver is used to replete glycogen stores and a smaller fraction is diverted towards lipogenesis, glycolysis, and oxidation (15).

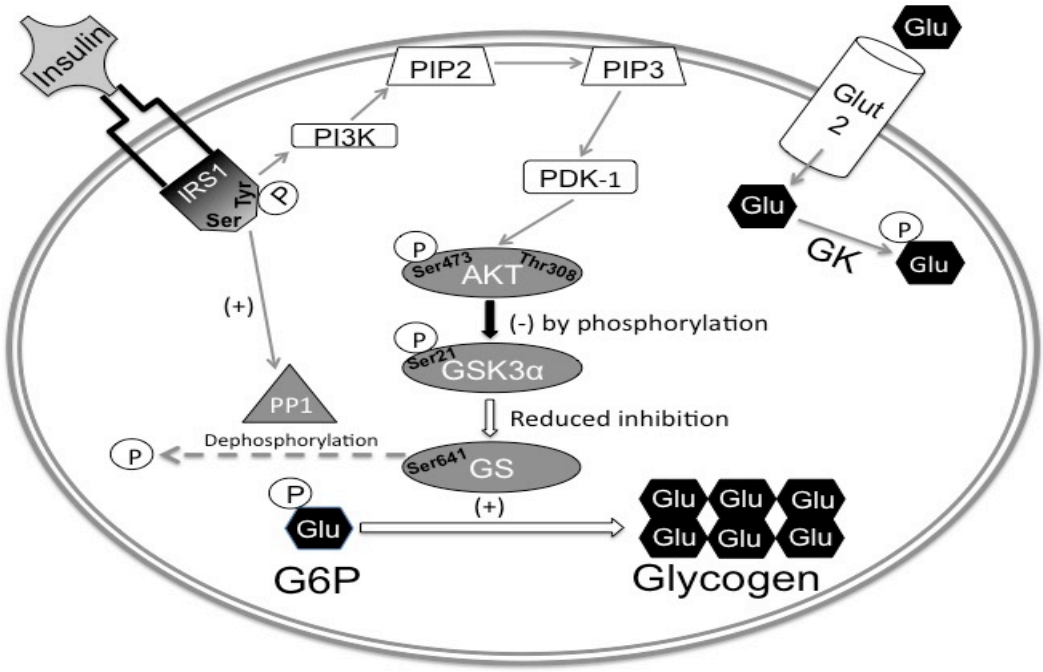

Figure 1. Schematic of insulin-mediated hepatic glycogen synthesis. Insulin binds to its receptor leading to autophosphorylation of the receptor. This promotes the interaction of the insulin receptor with the insulin receptor substrate 1 (IRS1) which is then phosphorylated at its tyrosine residue. Subsequently, phosphatidylinositol 4,5-bisphosphate (PIP2) is converted to phosphatidylinositol (3,4,5) trisphosphate (PIP3) through phosphoinositide 3-kinase (P13K)-mediated phosphorylation. PIP3 activates phosphoinositide-dependent kinase-1 (PDK-1), which promotes phosphorylation of AKT at Ser^{473}. Activated AKT phosphorylates glycogen synthase kinase 3α (GSK3α) at Ser21 to shut down the inhibitory effect of GSK3α on glycogen synthase (GYS). Through a series of reactions, insulin concomitantly activates PP1, which dephosphorylates GYS on the Ser^{641} residue, allowing GYS to actively convert G6P to glycogen.

2.2.2 Regulation of Glycogen Synthesis

GYS is the rate-limiting enzyme of glycogen synthesis and is present in two known isoforms; glycogen synthase 1 (GYS1) and glycogen synthase 2 (GYS2). These isoforms are found in muscle and liver, respectively and are known to be regulated by both allosteric and covalent mechanisms (19, 20). Allosteric regulation involves the binding of an “effector” (e.g. G6P) to a site other than the active site of the enzyme. This binding results in a conformational change of the protein, thereby modifying its activity. This regulatory mechanism elicits a rapid response to high substrate concentrations since it does not rely on hormonal signaling. With respect to GYS, high intracellular concentrations of G6P are known to allosterically activate this enzyme (19). On the other hand, covalent regulation involves the covalent attachment/removal of a molecule (e.g. phosphate group) to an enzyme, usually in response to a hormonal signal. Likewise, this in turn leads to conformational changes that alter the activity of the enzyme. Covalent regulation of GYS occurs through kinases or phosphatases which inhibit and promote GYS activity respectively (21). These include PKA, AMP-activated protein kinase (AMPK), GSK3, and PP1.

The rate of incorporation of glucose into glycogen in the liver is directly correlated with GYS2 activity (19). High G6P concentrations have been shown to override covalent modification and activate GYS2 through allosteric mechanisms. Given the blunted rate of glycogen synthesis in patients with diabetes and liver pathologies, there has been an increased focus on methods to promote GYS activity. These patients often see impaired GYS regulation due to their inability to respond to insulin. However, the challenge lies behind activating GYS without

compromising alternate metabolic pathways such as glycogenolysis, which is critical when glucose availability is scarce.

For instance, one approach to promoting allosteric activation of GYS has been to increase the intracellular concentration of G6P by increasing glucokinase (GK) content and activity. This enzyme phosphorylates incoming glucose to form G6P. It has been reported that in both fasted and fed animals, overexpression of GK results in significantly higher glucose phosphorylation in the liver. In fed animals, higher doses of GK overexpression resulted in significant reduction in circulating glucose and greater than 65% reduction in circulating insulin concentrations. Despite effectively clearing glucose from the blood, the rate of glycogen synthesis was not measured and no difference in glycogen content was found in the fed state (22). Therefore, the fate of G6P in this study is uncertain. To this end, primary hepatocytes overexpressing GK have shown significant increases in glycogen synthesis. Despite being successful in glucose clearance from the blood, overexpression of GK increases circulating triglycerides (TAG) and non-esterified fatty acids (NEFA) by 190% and 310%, respectively (22). Therefore, the elevated levels of NEFA and TG negate the benefits of improved glycemia.

Another kinase, which has importance in GYS activity in the liver, is AMPK. AMPK activity has also been studied extensively as a covalent regulatory mechanism. It is an energy-sensing protein that is activated under conditions of low energy levels to promote energy production pathways while inhibiting anabolic processes. Moreover, it is involved in a number of metabolic pathways including lipid/protein synthesis, cell growth, and mitochondrial biogenesis (23).

Isolated hepatocytes from overnight fasted rats have been incubated with AICAR (a known pharmacological activator of AMPK) and glucagon (a known activator of glycogenolysis) to study GYS activity. Glucagon elicited rapid (within 5 min) inactivation of GYS2 and activation of glycogen phosphorylase (GP) activity. On the other hand, AICAR induced AMPK activation and led to more gradual phosphorylation of GYS2 at Ser^7 (site 2) on the NH_2-terminal and a concomitant increase in glycogen phosphorylase (GP) activity (24). The same group went further and studied mice lacking the α1 and α2 catalytic subunits of AMPK (AMPKα1/α2-KO) in an attempt to investigate the contribution of AMPK to GYS activity. Basal GYS activity of AMPKα1/α2-KO mice was 2-times greater than in their wild-type counterparts. However, treatment of these mice with glucagon revealed a similar reduction of GYS activity compared to WT. These results suggest a possible pharmacological target of liver specific AMPK activity to promote glycogen synthesis.

Recent studies have attempted to target proteins immediately involved in the glycogen synthesis pathway rather than targeting upstream proteins with less specificity. As such, the interest in direct GYS regulation has sparked a lot of attention given that it is the terminal enzyme of glycogen synthesis. Accordingly, another approach to facilitating glucose clearance and storage has been to induce hepatic overexpression of a constitutively active form of glycogen synthase. When studying the ability to clear glucose from the blood using a intraperitoneal glucose tolerance test (IPGTT), rats with mutated phosphorylation sites 2 and 3B on GYS were significantly better at clearing glucose from the blood and had a 30% smaller AUC compared to wild type (25). Rats expressing

constitutively active GYS had a two-fold increase in glycogen content under fed states compared to their wild type counterparts (25). This finding suggests that the limiting factor to glycogen synthesis is not the storage capacity or number of enzymes itself, but rather the activation state of existing enzymes. Moreover, they had less glycogen stores when fasted compared to their fed state indicating the mobilization of glycogen under fasting conditions despite having the mutated GYS. This approach has been deemed successful in lowering blood glucose in fed states (25). Additionally, rats with mutated GYS showed no difference in circulating insulin, lactate, NEFAs, or TAGs.

2.2.3 Glycogenolysis

The storage of glycogen is a process that not only minimizes the elevation of blood glucose levels, but also prepares the system for fasting conditions. When glucose availability is scarce, and circulating insulin levels are low, glycogen stores can be mobilized through glycogenolysis to normalize plasma glucose concentrations. Normally, this contributes to ~ 75% of resting blood glucose (14). However, in the case of diabetes and insulin resistance, this mechanism becomes a deregulated and ongoing event contributing to a hyperglycemic state.

Normally, upon fasting or during an exercise stimulus, both glucagon and epinephrine are elevated to mobilize glycogen stores and normalize blood glucose concentrations. Although both are important mediators of glycogenolysis in muscle, glucagon; the counter-regulatory hormone to insulin is the major stimulator of glycogen breakdown in the liver with epinephrine having a

potentiating effect. Once a ligand binds to a G-Protein coupled receptor (GPCR) (i.e. β-Adrenergic and glucagon receptors for epinephrine and glucagon, respectively) the GPCR undergoes a conformational change. As a result, the α subunit of the GPCR exchanges GDP for GTP and dissociates from the GPCR to migrate to and activate adenylate cyclase. Activated adenylate cyclase uses adenosine triphosphate (ATP) to produce cyclic adenosine monophosphate (cAMP), which acts as a second messenger to activate protein kinase A (PKA). Elevated cAMP aids in dismantling the tetrameric inactive PKA (consisting of 2 catalytic and 2 regulatory subunits) and freeing the catalytic subunits. Activation of PKA leads to the subsequent phosphorylation and activation of phosphorylase kinase (PK). Ultimately, phosphorylase kinase phosphorylates and activates glycogen phosphorylase (GP), which catalyzes the breakdown of glycogen into glucose 1-phosphate (G1P) monomers (26).

The rate of glycogen breakdown is in part dependent on the activity of glycogen phosphorylase, which similar to GYS, appears to involve covalent and allosteric regulatory mechanisms. In a fed state, high circulating insulin inhibits glycogen catabolism in an attempt to minimize elevations in postprandial glycemia. Through a series of reactions, insulin activates Protein Phosphatase 1 (PP1), which subsequently dephosphorylates and inactivates glycogen phosphorylase (27). Moreover, insulin also activates Phosphodiesterase (PDE), which converts cAMP to AMP, thereby removing the second messenger mediated signaling for glycogenolysis. Glycogen metabolism is thus a tightly regulated process influenced by a number of hormones and substrates depending on the nutritional status of the system (26).

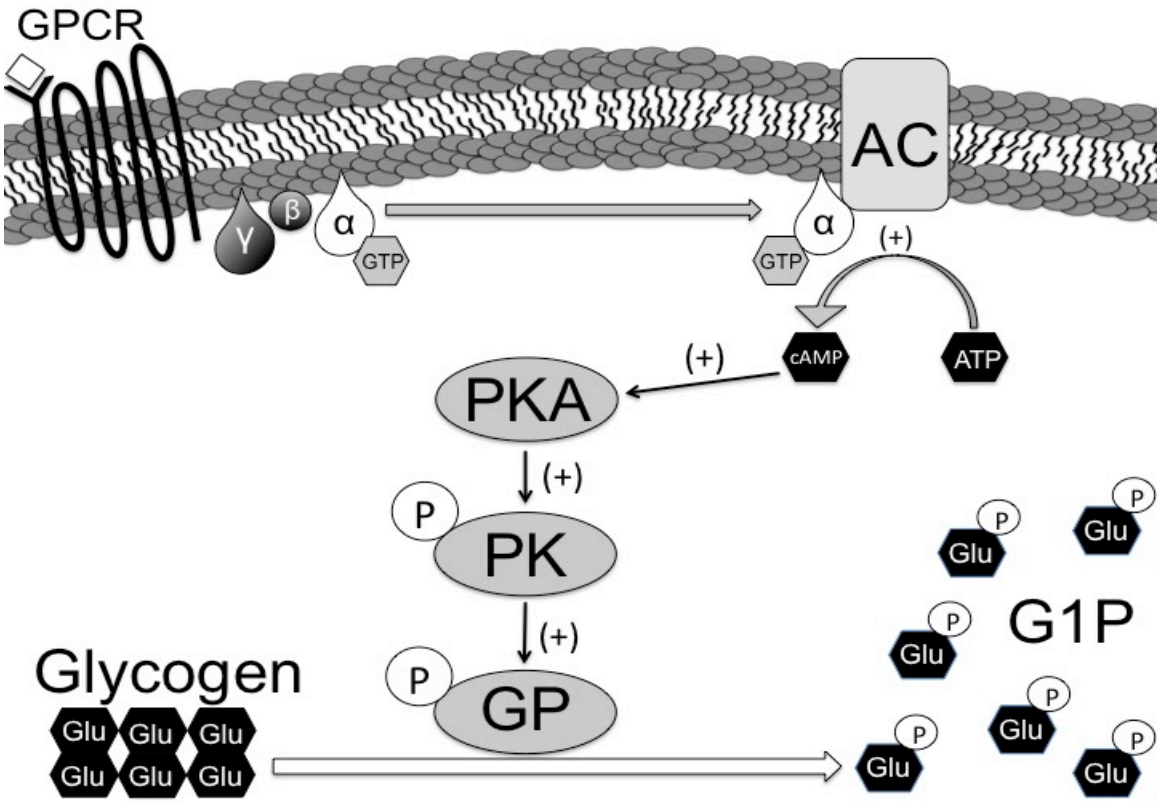

Figure 2. Schematic of glucagon/epinephrine-mediated glycogenolysis. A ligand (glucagon/epinephrine) binds to the G-Protein Coupled Receptor (GPCR) leading to a conformational change of the receptor. Subsequently, the α subunit is activated upon exchanging its guanosine diphosphate (GDP) for guanosine triphosphate (GTP). The α subunit migrates towards and activates adenylate cyclase (AC). AC converts adenosine triphosphate (ATP) to the second messenger cyclic adenosine monophosphate (cAMP) which serves to activate Protein Kinase A (PKA). Activated PKA phosphorylates phosphorylase kinase (PK), which subsequently phosphorylates glycogen phosphorylase (GP). Activated GP catalyzes the breakdown of glycogen into glucose 1-phosphate (G1P).

2.2.4 Gluconeogenesis (GNG)

Given the importance of the liver in blood glucose regulation, it is imperative that tightly regulated mechanisms are in place to maintain euglycemia in a state of fasting and post-glycogen depletion. In times when glucose availability is inadequate, the body is able to synthesize glucose from non-carbohydrate sources including lactate, pyruvate, alanine, and glycerol. This *de novo* synthesis of glucose is referred to as gluconeogenesis (GNG), a process that occurs almost exclusively in the liver. GNG is usually activated 4-6 hours after the onset of fasting and is at its maximal output upon complete depletion of glycogen stores (28). *De novo* production of glucose is primarily stimulated by glucagon and catecholamines while being inhibited by insulin.

2.2.4.1 Mechanism of GNG

The mechanism by which the liver produces glucose involves the reciprocal reactions of glycolysis with the exception of three notable differences (Figure 3).

1. Oxaloacetate (OAA) → Phosphoenolpyruvate (PEP)
2. Fructose 1-6 Bisphosphate (FBP) → Fructose 6 Phosphate (F6P)
3. Glucose 6-Phosphate (G6P) → Glucose

As a result of these differences, the glycolytic enzymes pyruvate kinase, phosphofructokinase, and hexokinase/glucokinase are replaced with phosphoenolpyruvate carboxykinase (PEPCK), fructose-1,6-bisphosphatase (FBPase) and glucose-6-phosphatase (G6Pase) respectively .

Under conditions of low circulating insulin and elevated glucagon or catecholamines, the liver actively converts any circulating lactate or alanine into pyruvate within the mitochondria. The resulting pyruvate is converted to OAA by pyruvate carboxylase (PC). The subsequent decarboxylation and phosphorylation of OAA by PEPCK is the first difference between glycolysis and GNG. In certain species, which lack mitochondrial PEPCK, OAA needs to be shuttled out of the mitochondria where it is converted to PEP by cytosolic PEPCK. Given that such transport mechanisms fail to exist for OAA, it is reduced to malate within the mitochondria. Malate is shuttled out through the malate aspartate shuttle (MAS) and oxidized back to OAA in the cytoplasm. In this case, OAA becomes a substrate for cytoplasmic PEPCK (PEPCK-C), an energy consuming process in the form of GTP. The resulting phosphoenolpyruvate (PEP) becomes 2-Phosphoglycerate (2-PG) with the help of enolase. 2-PG proceeds further into the GNG pathway and forms 3-Phosphoglycerate (3-PG); a reaction catalyzed by phosphoglycerate mutase (PGAM). Next, intracellular 3-PG forms 1,3-BPG with the help of phosphoglycerate kinase (PGK). The resulting 1,3 BPG is a substrate for the enzyme glyceraldehyde phosphate dehydrogenase (GAPDH) to produce glyceraldehyde 3-phosphate (G3P). Subsequently, G3P yields fructose 1-6 bisphosphate in a reaction catalyzed by aldolase.

The second difference lies in the conversion of fructose 1-6-bisophosphate to fructose 6-phosphate by removal of a phosphate group on its first carbon; catalyzed by fructose 1-6 biphosphatase. Then, phosphohexoisomerase (PHI) catalyzes the reversible reaction of fructose 6-phosphate to G6P (15).

The final distinction and rate-limiting step of this pathway lies in the conversion of G6P to glucose by G6Pase. This step removes a phosphate group from G6P, which was originally incorporated by glucokinase. As a result, glucose is no longer bound intracellularly and is free to exit the cell and find its way to extrahepatic tissues.

Unlike pyruvate, lactate, and alanine, glycerol enters the GNG pathway at a later stage. Glycerol is converted to G3P by glycerol kinase (GLYK), after which it will undergo the same fate as the other precursors in the synthesis of glucose.

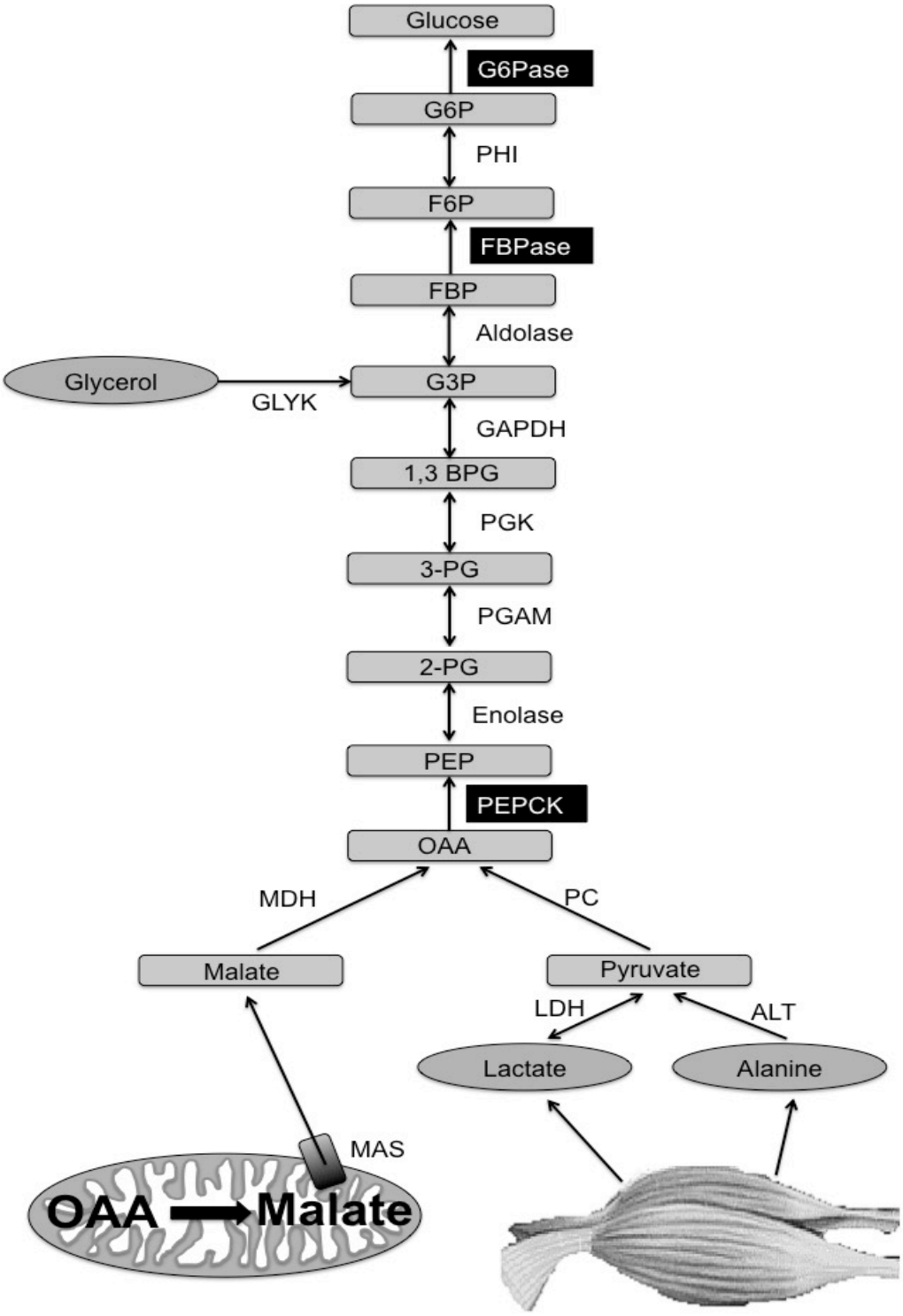
Glucose
G6Pase
G6P
PHI
F6P
FBPase
FBP
Aldolase
Glycerol
GLYK
G3P
GAPDH
1,3 BPG
PGK
3-PG
PGAM
2-PG
Enolase
PEP
PEPCK
OAA
MDH
PC
Malate
Pyruvate
LDH
ALT
Lactate
Alanine
MAS
OAA
Malate

Figure 3. Schematic of the gluconeogenic pathway. Lactate and alanine are converted to pyruvate by lactate dehydrogenase (LDH) and alanine transaminase (ALT) respectively. Pyruvate and malate (shuttled out of the mitochondria by the malate aspartate shuttle (MAS)) become Oxaloacetate (OAA) by malate dehydrogenase (MDH) and pyruvate carboxylase (PC) respectively. OAA proceeds up the GNG pathway through the reverse reactions of glycolysis with the exception of three reactions. 1) OAA to phosphoenolpyruvate (PEP), 2) fructose 1,6-bisphosphate (FBP) to fructose 6-phosphate (F6P), and 3) glucose 6-phosphate (G6P) to glucose are catalyzed by phosphoenolpyruvate carboxykinase (PEPCK), fructose 1,6-bisphosphatase (FBPase), and glucose 6-phosphatase (G6Pase) respectively. Glycerol enters in the later stages of GNG and is converted to glyceraldehyde 3-phosphate (G3P) by glycerol kinase (GLYK). Other abbreviations include 2-phosphoglycerate (2-PG), phosphoglycerate mutase (PGAM), 3-phosphoglycerate (3-PG), phosphoglycerate kinase (PGK), 1,3-bisphosphoglycerate (1,3 BPG), glyceraldehyde phosphate dehydrogenase (GAPDH), fructose 1,6-bisphosphate (FBP), and phosphohexoisomerase (PHI).

2.2.4.2 Peroxisome proliferator-activated receptor (PPAR)-γ co-activator-1α (PGC-1α)

PGC-1α is a transcriptional co-activator and has various tissue dependent effects. It has been shown to be crucial for mitochondrial biogenesis in muscle, and thermogenesis in brown adipose tissue, whereas in the liver the primary role of PGC-1α is to regulate the expression of gluconeogenic genes (29, 30). Importantly, it has been reported that the activity of PGC-1α is deregulated in both NAFLD as well as diabetes (29–32). In the presence of low circulating insulin or insulin resistance, PGC-1α expression is increased. Conversely, when circulating insulin is high (in a fed state), the expression of PGC-1α is rapidly reduced. The mechanism behind PGC-1α regulation is not completely understood. It appears that an elevation in glucagon and glucocorticoids may directly promote PGC-1α expression. Along the same lines, it has been suggested that elevations in insulin directly inhibit the effects of glucagon on the PGC-1α promotor region. Despite this, although PGC-1α is important for GNG, this protein requires a number of transcription factors to be present in order to elicit its effects (28, 33, 34).

Yoon et al, provided important mechanistic insight into the role of PGC-1α in GNG. By treating mice with streptozotocin (STZ), they were able to mimic the physiological parameters of type 1 diabetics. These mice show constantly elevated hepatic expression of PGC-1α, consistent with the view that the content of this protein is increased under conditions of insulin deficiency (35). The same group used a fasting/re-feeding model to demonstrate that the increased hepatic PGC-1α expression in the fasted state is followed by elevated PEPCK and G6P

content shortly after; supporting the notion that PGC-1α expression precedes the activation of gluconeogenic genes in the liver. Conversely, re-feeding resulted in a down regulation of PGC-1α expression and a concomitant reduction in hepatic PEPCK/G6P content (31).

In contrast to their insulin-centered experiments, the same group went further to investigate the glucagon/epinephrine mediated effects on PGC-1α. Normally, hepatic cAMP is elevated in the fasted state. Moreover, it has been shown that cAMP acts through β-adrenergic receptors to promote PGC-1α expression in brown fat where it is crucial for the thermogenic properties of brown fat (36). Under the same principle, primary hepatocytes were stimulated by 8-bromo-cAMP, a cAMP analogue. This study found that stimulation by 8-bromo-cAMP elicited a large increase in PGC-1α mRNA (31). As such, elevations in cAMP in a fasted state promotes the expression of PGC-1α mRNA. This is one mechanism behind elevated GNG upon fasting.

2.2.4.3 PEPCK

Phosphoenolpyruvate Carboxykinase (PEPCK) is a rate-limiting enzyme in GNG and is largely present in hepatocytes in both mitochondrial (PEPCK-M) and cytosolic (PEPCK-C) isoforms. Although humans possess relatively equal amounts of both isoforms, rodents express up to 90% PEPCK-C, which limits the research in these animals almost entirely to this isoform (37, 38). As illustrated by Hanson et al., liver-specific as well as whole-body PEPCK knockout mice elicit severe hypoglycemia and even death in as little as two days after birth. Moreover, mice lacking PEPCK had 2-3-fold more hepatic triglyceride content

and 50% more circulating triglycerides compared to controls (38). This increase in triglycerides has been attributed to a 10-fold increase in hepatic malate concentration, which disrupts the Krebs cycle. The backup of Krebs cycle intermediates promotes a buildup of acetyl-CoA, reduced fat oxidation, and a buildup of hepatic triglycerides (38). Therefore, it is clear that proper regulation of PEPCK is critical for both GNG and lipid metabolism.

Unlike proteins in the glycogen synthesis cascade, PEPCK activity is regulated at a transcriptional level rather than covalent modification. Under basal conditions when insulin levels are low, and glucagon levels are elevated (resulting in elevated cAMP), transcription of PEPCK is increased. This results in greater conversion of OAA into PEP, which promotes hepatic glucose production. Conversely, in a fed state, PEPCK activity is suppressed in response to elevated insulin and reduced glucagon concentrations (39).

Although transcription of PEPCK is regulated through hormones, these hormones elicit their effects through a number of transcription factors (e.g. Forkhead box protein O1 *(*FOXO1*),* Hepatocyte nuclear factor 4α (HNF4α), and Peroxisome proliferator-activated receptor *α* (PPARα)) and the transcriptional co-activator PGC-1α. These factors serve to promote transcription of GNG genes including PEPCK and G6Pase. Transcription factors such as FOXO1 and HNF4α bind to the promoter regions adjacent to a specific gene of interest, thereby controlling the rate of transcription for that gene. In addition, co-activators such as PGC-1α, promote gene expression by binding to transcription factors, as co-activators are unable to bind directly to the DNA sequence themselves (28, 31, 33) .

Rhee et al., provided valuable insight into the importance of HNF4α in GNG gene transcription. By analyzing RNA taken from either control or liver-specific HNF4α-KO mice, they found that under fasting conditions, HNF4α-KO mice fail to express PEPCK or G6Pase to the same extent seen in control mice. Intriguingly, in both fed and fasted states, PGC-1α expression was greater in HNF4α-KO than controls. It is not clear whether this is a compensatory mechanism resulting from compromised GNG, or whether HNF4α itself plays a role in the regulatory mechanisms of PGC-1α that are compromised with HNF4α-KO. Furthermore, the same group was interested in whether HNF4α is critical for PGC-1α to elicit its effects. In this respect, they isolated primary hepatocytes that were either controls or KO for HNF4α. Using adenoviral infection of PGC-1α in control livers resulted in a concomitant rise in PEPCK and G6Pase expression. However, similar mRNA infection of PGC-1α in HNF4α-KO hepatocytes fails to express these GNG genes. As a result it is clear that HNF4α plays a critical role in the transcription of GNG genes that cannot be carried out by PGC-1α alone (28).

FOXO1 is another transcription factor involved in GNG that appears to be regulated in an insulin-dependent manner. That is, upon insulin binding to its receptor, phosphorylated AKT later phosphorylates FOXO1 leading to the exclusion of this transcription factor from the nucleus (33, 40). Upon exclusion from the nucleus, FOXO1 is unable to engage in gene transcription. However, under fasting conditions, or in T2D where insulin action is reduced or impaired respectively, reduced phosphorylation of AKT leaves FOXO1 permeable to the nucleus. This permits FOXO1 to partake in GNG gene transcription in

conjunction with PGC-1α. Yoon et al., used FAO hepatoma cells to study the interaction of PGC-1α and FOXO1. FAO hepatoma cells have very little endogenous PGC-1α and are therefore a viable model to study this protein using adenoviruses. It has been reported that when infected with PGC-1α alone, these cells display concomitant rises in G6Pase and PEPCK expression. However, when infected with a truncated FOXO1 allele (also a dominant negative suppressor of wild type FOXO1) or PGC-1α in conjunction with the truncated FOXO1 allele, expression of these GNG genes is heavily compromised. Therefore, it appears that the functional interaction of PGC-1α with FOXO1 is critical to the induction of GNG genes (33, 40).

2.2.5 Glucose 6-Phosphate

Glucose 6-Phosphate (G6P) is a unique intermediary molecule in glucose metabolism because of its versatility in the preservation of glycemic control. Upon entering a hepatocyte, glucose is rapidly phosphorylated by GK, which prevents it from exiting the cell. The resultant G6P is now readily available for storage in a state of hyperglycemia (41). In contrast, G6Pase is capable of reversing the initial reaction catalyzed by GK, thus liberating glucose into circulation under conditions of hypoglycemia. Therefore, the fate of G6P may be determined by four factors. These include the concentration of 1) glucose and 2) G6P available at a cellular level and the enzymatic activity of both 3) GK and 4) G6Pase.

2.3 Hepatic Lipid Metabolism

Similar to carbohydrates, lipids represent a crucial source of energy particularly under fasting conditions. Given that they contain more than twice the energy content of carbohydrates and proteins, lipids are a highly efficient energy source. Hepatic regulation of incoming lipids maintains lipid homeostasis as the liver packages incoming fats into very-low-density-lipoproteins (VLDL) and exports them to peripheral tissues. As the newly synthesized VLDLs circulate past muscle and adipose tissues, lipoprotein lipase (LPL) cleaves TAGs contained in the VLDL to liberate fatty acids (FA) for oxidation or re-esterification. Analogous to how the body stores glucose as glycogen; FAs are preferentially stored as triglycerides within the adipose tissue. Under fasted conditions, rates of FA oxidation are increased in an attempt to minimize glucose oxidation and promote GNG. This ensures that glucose is spared for glucose-dependent organs such as brain. However, in a state of glucose abundance, the body preferentially oxidizes glucose and suppresses fat oxidation (42).

2.3.1 Lipogenesis

Given that the glycogen stores in both liver and muscle are limited and that the liver is the central regulator of glycemia, there are mechanisms in place to deal with surplus carbohydrates. Under, these conditions, when circulating insulin is elevated, the body converts excess carbohydrates into fat, a process known as lipogenesis. Insulin serves to increase the activity of enzymes catalyzing lipid synthesis while concomitantly inhibiting those catalyzing lipid breakdown (15).

Subsequent to a high carbohydrate diet, the primary means of dealing with the abundance of glucose is to store it as glycogen. Any remaining glucose will undergo glycolysis, be converted to glycerol 3-phosphate (required for esterification of fatty acids to form TAG), or lipogenesis (Figure 4). Once glucose enters the cell and undergoes glycolysis within the cytoplasm, the resulting pyruvate molecules enter the mitochondria. Pyruvate dehydrogenase (PDH) converts pyruvate into acetyl-CoA. Although acetyl-CoA is a precursor of fat synthesis, it cannot be used for lipogenesis as long as it remains in the mitochondria. Therefore the body must shuttle this molecule across the mitochondrial membrane and into the cytoplasm where many of the enzymes required for *de novo* lipid synthesis are located. Given that the mitochondrial membrane is impermeable to acetyl-CoA, and there are no active shuttles to transport it into the cytoplasm, it enters the Krebs cycle. Once in the Krebs cycle, acetyl-CoA (2C) and OAA (4C) fuse to form citrate (6C) in a reaction catalyzed by citrate synthase. Unlike acetyl-CoA, citrate can cross the mitochondrial membrane and gain access into the cytoplasm, where it will be broken down again into OAA and acetyl-CoA. This reaction is catalyzed by ATP-Citrate Lyase (ACYL). The resultant cytoplasmic acetyl-CoA is carboxylated in the presence of insulin by acetyl-CoA carboxylase (ACC) into malonyl-CoA (43). This newly synthesized malonyl-CoA is a potent inhibitor of carnitine palmitoyltransferase I (*CPT1*). Through a series of condensation reactions, which add 2 carbons each time to malonyl-CoA, a fatty acid (i.e. palmitate or oleate) is synthesized. This reaction occurs with the aid of fatty acid synthase (FAS). The newly synthesized

fatty acids are esterified to glycerol phosphate to form TAG. The latter are packaged into VLDLs and released into circulation (44, 45).

Insulin is a potent stimulator of *de novo* lipogenesis. Moreover, the rate of lipogenesis depends largely on the availability and activity of two major enzymes; namely ACC and FAS. These enzymes are regulated at the level of transcription, depending on nutritional status. Sterol regulatory element-binding protein-1c (SREBP-1c) is believed to be the master regulator of gene transcription for enzymes involved in the *de novo* lipid synthesis pathway. In the fed and fasted states, SREBP-1c expression is elevated and suppressed respectively (46). To illustrate the importance of this transcription factor in lipogenesis, mice with liver specific overexpression of SREBP-1c have been studied. Overexpression of this factor promotes the development of fatty livers by 24 weeks of age. Moreover, these mice display 50% more fatty acids stored in the liver compared to controls. This occurred even in mice fed a standard chow (SC) diet. Moreover, SREBP-1c overexpression revealed a two-fold increase in FFA and TAG in addition to a three-fold increase in insulin in the blood (47).

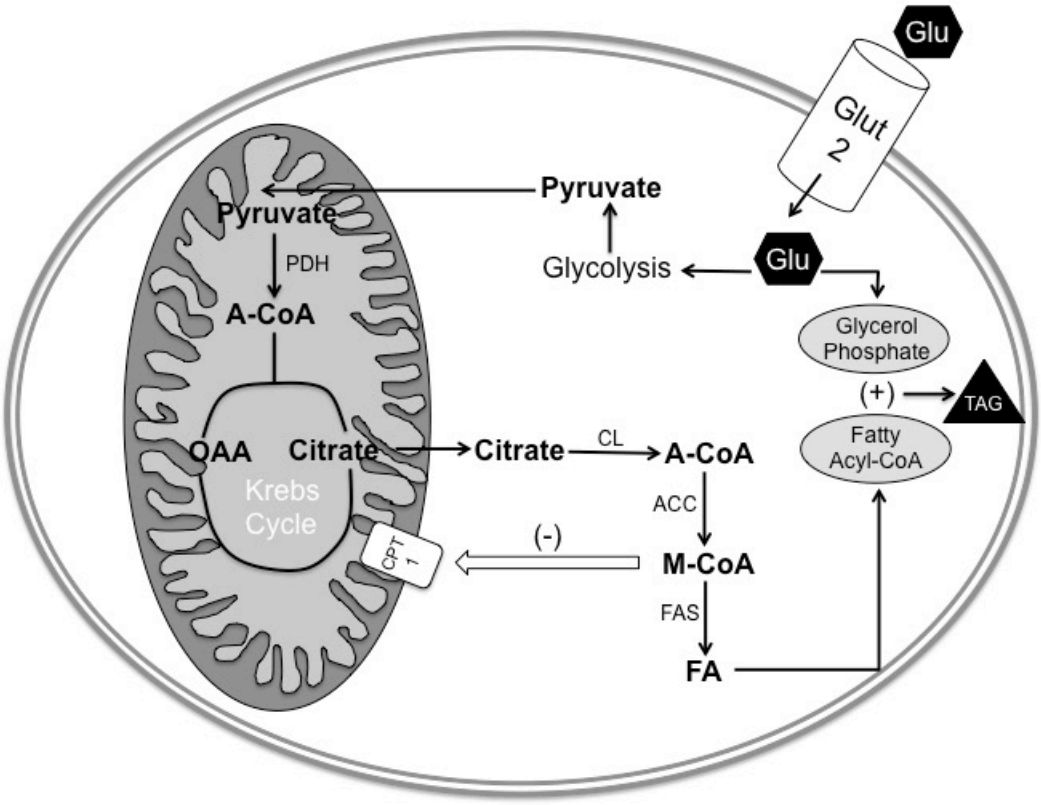

Figure 4 - Schematic of de novo lipogenesis in a liver cell. Upon a high influx of glucose into the cell, glucose undergoes glycolysis or forms glycerol phosphate. Pyruvate from glycolysis enters the mitochondria and is converted to acetyl-CoA (A-CoA) by pyruvate dehydrogenase (PDH). Pyruvate enters the Krebs cycle and exits the mitochondria as citrate. Citrate lyase (CL) converts citrate to A-CoA. In the presence of insulin, acetyl-CoA carboxykinase (ACC) is dephosphorylated and activated. ACC converts A-CoA to malonyl-CoA (M-CoA). M-CoA is formed into a fatty acid by fatty acid synthase (FAS). This is accomplished by continuously adding 2 carbons through a series of condensation reactions. The newly formed fatty acyl-CoA is esterified to glycerol phosphate to yield a triglyceride (TAG) (44, 45).

2.3.2 Lipid Oxidation

Under fasting conditions, or when circulating insulin levels are low and glucagon is elevated, the body mobilizes its fat stores within the adipose tissue. Stored triglycerides are actively hydrolyzed into FFA, which are then released into the bloodstream. These FFA eventually reach the mitochondria, peroxisomes, or endoplasmic reticulum of muscle and liver to undergo oxidation. Normally, the rate of hepatic FAO is proportional to the plasma concentration of FFA released by the adipose tissue (48).

The oxidation of fatty acids can be thought of as a three step process involving 1) Activation, 2) Transport, and finally 3) Oxidation. Aside from some short and medium chain fatty acids, long chain fatty acids are impermeable to the mitochondrial membrane. As a result, fatty acids are “activated” by converting them into acyl-CoA molecules within the cytoplasm. This is catalyzed by the enzyme fatty acyl-CoA synthetase (FACS). The resulting long chain acyl-CoA molecules are “transported” into the mitochondria, the primary site of β-oxidation, by CPT1 (49). This translocase is located on the outer mitochondrial membrane. CPT1 fuses the acyl group from acyl-CoA with carnitine to make it transportable into the mitochondria. Hence, CPT1 acts as a gatekeeper and is therefore a rate-limiting transporter in the oxidation of long chain fatty acids (LCFA). Inhibition of CPT1 (by malonyl-CoA, an intermediary molecule of lipogenesis) limits fat oxidation to short-chain fatty acids, which can freely diffuse through the mitochondrial membrane. Once in the mitochondria, fatty acids undergo β-oxidation resulting in the cleaving of fatty acids into 2-carbon acetyl-CoA

molecules. The resulting acetyl-CoA may enter the Krebs cycle to undergo further oxidation, or be converted to ketone bodies and which can then enter circulation.

2.4 Regulation of Glucose and Lipid Metabolism

The regulation between lipid and carbohydrate metabolism was first described by Philip Randle who stressed the reciprocal regulation of these two macromolecules under various nutritional states (50). In a fed state, when circulating insulin is high and glucagon levels are low, glucose oxidation is promoted while fat oxidation is inhibited. In fact, under these conditions, the synthesis of fats from excess glucose involves a concomitant rise in malonyl-CoA that is later converted to fatty acids by the ACC/FAS pathway. Elevated malonyl-CoA exerts an allosteric inhibitory effect on CPT1 and channels fatty acids towards TAG synthesis. This prevents the redundant process of allowing newly synthesized acyl-CoA molecules from subsequently undergoing β-oxidation. On the other hand, in a fasted state with low insulin and elevated glucagon, malonyl-CoA levels are down which lifts its allosteric inhibition on CPT1 (50). This allows β-oxidation and the liberation of ATP from fatty acids, while concomitantly preserving glucose for glucose dependent tissues.

2.5 High-Fat Diet

HFDs (which contain up to 60% of calories from fats in extreme cases), particularly those rich in saturated fats are known to induce dyslipidemia, hyperinsulinemia, and hyperglycemia. Normally, fats are preferentially stored within the white adipose tissue (WAT) in the form of TAG. When feeding a HFD, the amount of fat available is so large that it exceeds ability of the WAT to store them (51). This results in hepatic lipid accumulation and disrupts normal liver function, which severely compromises the ability of this organ to properly maintain glucose and lipid homeostasis. It is unclear whether hepatic insulin resistance precedes or is a result of excessive accumulation of lipids in the liver (52). However, what seems to be well established is that prolonged exposure to a HFD leads to several metabolic abnormalities including increased lipolysis, impaired glucose disposal, and elevated hepatic GNG and glycogenolysis (40, 53, 54).

2.5.1 Mechanism(s) of HFD-induced Hepatic Insulin Resistance

Although the mechanism(s) underlying the development of hepatic insulin resistance is not fully understood, some advances in this field have been made in recent years. In this context, the excessive accumulation of lipids in hepatocytes as a result of HF feeding has been considered a major factor in the development of hepatic insulin resistance. A well-described mechanism involves the increase in the intracellular concentration of diacylglycerols (DAG), which lead to the activation of protein kinase C (PKC). The latter is well known for its ability to phosphorylate serine residues of IRS-1, which prevents the induction of IRS-1

phosphorylation at tyrosine residues by the insulin receptor (55). This leads to inhibition of the downstream signaling events by which insulin regulates glucose metabolism in the liver. This is well illustrated in mice with liver-specific deletion of the PKC gene that display improved insulin sensitivity, despite having elevated hepatic lipid content under HF-feeding conditions (56).

2.5.2 Fatty Acid Induced increase in Gluconeogenesis

Chronic HF-feeding has been associated with dyslipidemia and elevated circulating NEFAs (57) as a result of insulin resistance (58). This increase in circulating NEFAs results in greater delivery of fats to the liver on top of the already excessive dietary fats. Moreover, it has been reported that hepatic GNG is elevated following chronic HF-feeding (59, 60). The underlying mechanism seems to involve an elevation in acetyl-CoA, NADH, and ATP resulting from increased fat oxidation. Acetyl-CoA is an allosteric activator of pyruvate carboxylase, an enzyme that adds a carboxyl group to pyruvate to form oxaloacetate. Oxaloacetate can then be acted on by PEPCK, feeding forward into the GNG pathway. Next, higher levels of NADH facilitate the conversion of 1-3 bisphosphoglycerate to glyceraldehyde 3-phosphate; once again leading towards glucose synthesis. Finally, ATP can be used in the energy-dependent steps of GNG.

Although the expected outcome would be that elevated GNG would also increase hepatic glucose output (HGO), the general consensus in the literature is that despite FFA increasing GNG within the liver, overall HGO remains unchanged in normal humans (61). Hepatic auto regulation is thought to be

involved, suggesting that upon sensing elevated GNG, some intra-hepatic compensatory mechanism (such as increased glycogen synthesis, reduced glycogenolysis, or both) prevents the concomitant rise in HGO (61). However, the mechanism by which this occurs is still poorly understood.

2.6 Non-Alcoholic Fatty Liver Disease (NAFLD)

NAFLD is known throughout the literature to be the hepatic manifestation of metabolic syndrome(62), and shown to be a better predictor of metabolic abnormalities than visceral adiposity (63). Over 90% of morbidly obese and 65% of T2D patients are diagnosed with NAFLD, a condition in which the patient's liver is composed of >5-10% fat (5). It encompasses a spectrum of liver pathologies from steatosis, to steatohepatitis, advanced fibrosis, and hepatocellular carcinoma. In fact ~ 20% of patients with non-alcoholic steatohepatitis (NASH) progress to fibrosis and eventually cirrhosis (6). Moreover, histological analysis of these patients' livers display similar characteristics to those of chronic alcohol consumers despite their alcohol intake being below the recommended guidelines(9). NAFLD impairs numerous metabolic parameters and insulin resistance, diabetes and obesity are significant pathophysiological factors in the manifestation of this condition (64). The fault apparently lies largely on the current North American HF and high-calorie diets in conjunction with certain advancements in technologies, which have steered both adults and children towards a more sedentary lifestyle (65).

2.6.1 Pathophysiology of NAFLD

Although the exact mechanisms involved in the pathogenesis of fatty liver disease are not completely understood, it is believed that increased visceral adiposity, elevated circulating NEFAs, and insulin resistance following HF feeding contribute to its manifestation (52). Due to the abundance in fat availability, adipose tissue dysfunction leads to an increase in the secretion of numerous inflammatory mediators such as tumor necrosis factor α (TNFα), interleukin 6 (IL-6), and nuclear factor kB (NFkB) (66, 67). TNFα has been shown to also promote serine phosphorylation of IRS-1, which inhibits the insulin-mediated tyrosine phosphorylation as previously described (68). Consequently, this leads to inhibition of downstream insulin-signaling pathways, which has been shown to be reversed in TNFα-KO mice (69). Next, with respect to IL—6, it has been reported that primary hepatocytes treated with IL-6 displayed less phosphorylation of AKT and a 75% reduction in glycogen synthesis (66).

Impaired insulin signaling through these inflammatory mediators compromise a number of metabolic pathways including lipolysis. Normally, insulin elicits an anti-lipolytic effect on adipose tissue, which becomes compromised in an insulin-resistant state (55). This results in increased release of NEFAs from the adipose tissue and higher delivery of these lipids to the liver(70). Importantly, the extra NEFAs released as a consequence of the impaired ability of insulin to suppress lipolysis contribute additional lipids to the already excessive amount that is incoming through the diet. Moreover, an elevation of lipogenic transcription factors and enzymes including SREBP-1c and FAS (12) have also

been reported. These factors have been attributed to increased *de novo* lipogenesis in an already steatotic liver (46, 47). Therefore, an overabundance of dietary fats in combination with increased lipolysis and elevated *de novo* lipogenesis are believed to eventually promote hepatic inflammation, leading to a downward spiral of metabolic disruptions.

2.6.2 Consequences of NAFLD

Individuals diagnosed with NAFLD, show elevated NEFAs, serum TAG, and serum LDL, regardless of whether they are diabetic or not (9). Also, it has been reported that this pro-athrogenic lipid profile observed in NAFLD is attributed primarily to insulin resistance (71). Mice with liver specific insulin receptor knockouts (LIKO) have been studied to better understand the deleterious effects of NAFLD-induced hepatic insulin resistance. Despite being on a standard chow diet, these mice reportedly have low levels of HDL. Moreover, VLDLs of these mice contained high levels of cholesterol rather than triglycerides. Within 12 weeks under these pro-athrogenic conditions, all LIKO mice developed severe atherosclerosis (71). From this it is clear that the detrimental effects of NAFLD stem far beyond the boundaries of the liver and elicit numerous systemic consequences.

Aside from the impairments in lipid metabolism, glucose metabolism has also been reported to be dysfunctional at the intra-hepatic and systemic levels. During a hyperinsulinemic-euglycemic clamp, Bugianesi et al., found that compared to normal subjects, those who were non-diabetic but had NAFLD elicited 30-45% less peripheral glucose disposal despite having normal HGP.

This was mainly attributed to impaired whole-body glycogen synthesis and glucose oxidation in these individuals. Furthermore, NAFLD subjects had significantly higher rates of lipid oxidation which was suppressed to a lesser extent in the presence of insulin when compared to controls(9). In a separate study, Marchessini et al., investigated insulin's ability to suppress HGP using the same clamp model. They found that the level of impairment in HGP suppression in NAFLD patients was similar to that of T2D. They also reported significantly less suppression of HGP compared to controls (8). This finding supports the notion that insulin resistance is a significant contributor to metabolic abnormalities resulting from NAFLD.

Finally, in its most pronounced stages, NAFLD has been shown to be associated with hepatocellular carcinoma and even liver failure (11). Moreover, serum aspartate transaminase (AST) and alanine transaminase (ALT), two markers of liver damage are significantly elevated in NAFLD patients (9).

2.7 Exercise

Healthcare professionals are prescribing exercise as a therapeutic tool to aid in the management of numerous metabolic conditions including obesity, T2D and NAFLD. Moreover, given that there are currently no approved therapies for NAFLD, exercise is one of two options available for its management. Studies have repeatedly shown improvements in glucose tolerance, insulin sensitivity, and blood lipid profiles in those who are physically active compared to sedentary individuals (13)(72). In fact it has been reported that in T2D patients there is

improved post-prandial glycemic control after as little as 7 days of aerobic exercise training (73).

Aerobic exercise is preferred over resistance training for improvement in metabolic efficiency. However one randomized control study comparing the effectiveness of aerobic vs. resistance training in NAFLD patients showed similar improvements in insulin sensitivity, hepatic fat content, and reversal of hepatic steatosis. Additionally, total body fat mass, visceral adiposity, and HbA1C (a marker of elevated blood glucose over last 3 months) levels were reduced in similar magnitudes between both aerobic and resistance-trained subjects (13).

Considering the implications that HF feeding has on NAFLD, the effects of exercise in conjunction with HF feeding has gained a lot of attention in recent years. HF feeding alone has been shown to induce a 2.2-fold increase in total hepatic lipid content. Interestingly, exercise was able to reverse the accumulation of intra-hepatic lipids by ~ 36%. Cintra et al, claim that the benefits in hepatic lipid content mobilization were associated with reduced SREBP-1c and FAS protein content (12). Moreover, these findings are further supported by Rabøl et al. who show that a single bout of exercise reduced *de novo* lipid synthesis by 30% and hepatic triglyceride synthesis by 40% (74).

The down regulation in SREBP-1c and FAS are likely due to improved insulin sensitivity. Insulin tolerance tests have reported that exercise improves glucose clearance from the blood by 41% in rats with diet-induced obesity (40).

Current literature focuses heavily on the acute (single bout) effects of exercise and/or HFD on glycemic control. These models give us some insight into the mechanisms of glycemic control and how they may be modified based on

acute lifestyle changes. However, they fail to portray the physiological adaptions seen from long-term adherence to exercise. Moreover, exercise is currently understood to be a long-term lifestyle intervention. Accordingly, our model of chronic HFD in conjunction with chronic exercise illustrates the benefits of a life-long adherence to training. Given that the last exercise bout is 48-hr prior to sacrifice, any changes we observe are due to actual metabolic alterations and not simply due to an acute exercise-induced stimulus.

3. Objectives and Hypotheses

In this context, **the objectives** of this thesis are twofold:

1) To determine whether endurance training reverses the deleterious metabolic effects of NAFLD by improving insulin signaling, increasing glycogen synthesis, and suppressing GNG in the liver
2) To investigate the potential molecular mechanisms by which endurance exercise improves hepatic glucose metabolism under basal and insulin-stimulated conditions.

The **hypotheses** to be tested are:

- That endurance exercise will increase fat oxidation, attenuate hepatic steatosis and improve whole-body glycemic control in HF-fed rats.
- That the HF-induced increase in PGC-1α and PEPCK in the liver will be reversed by endurance exercise.
- That endurance exercise will prevent the HF diet-induced impairment in insulin signaling in the liver and increase glycogen synthesis while suppressing GNG.

4. Experimental Design & Methods

4.1 Animals

All experimental procedures were subject to approval by the York University Animal Care Ethics Committee prior to beginning the study. Male albino rats from the wistar strain weighing ~200 g (initial weight) were maintained on a 12 h light (7:00-19:00) and 12 h dark (19:00-7:00) cycle and left to acclimatize for one week at 23° C. Upon acclimatization the rats were screened on three separate occasions for their willingness to exercise using an exercise selection protocol. This protocol began with a 5 min warm up period consisting of an inclination and speed of 5% and 10m/min respectively. After the warm up, treadmill inclination was raised to 10% for the remainder of the protocol and speed was increased by 2 m/min up to a maximum of 30m/min. Rats that were unable to run at a minimum speed of 20 m/min for 20 min on all 3 occasions were used as controls. Subsequent to the selection process, rats were randomly divided into 4 groups (n=8): sedentary standard chow (Sed SC), exercise standard chow (Ex SC), sedentary high-fat (Sed HF), and exercise high-fat (Ex HF). The animals' ad libitum food intake and body weight was measured on a daily basis. Both the SC and HF foods were obtained from Research Diets. The SC diet contained 70%, 10%, and 20% of the calories from carbohydrates, fat, and protein respectively. The HF diet contained 20.1%, 59.9%, and 20% of the calories from carbohydrates, fat and protein respectively.

4.2 Exercise Training Protocol

In order to set the training intensity, animals in the Ex SC and Ex HF groups underwent a peak VO_2 test using a treadmill connected to the Comprehensive Laboratory Animal Monitoring System (CLAMS). Once resting VO_2 was recorded, the 5-min-warm-up-period began (10 m/min, 0% inclination). The speed of the treadmill was then increased by 2m/min every two minutes thereafter. The test ended when the rats reached exhaustion (characterized by sitting on the shock pad for 5 seconds, plateau in VO_2, or RER of 1 or higher). Using the peak VO2 values, a protocol was designed to have the animals undergo chronic endurance training for 1 h/day, 5 days/week up to a maximum speed that corresponds to 70-85% of their peak VO_2. This was chosen due to the fact that it is the same intensity recommended by the American College of Sports Medicine (ACSM) for optimal health benefits in humans(75). Furthermore, VO_2 assessments were conducted bi-weekly so running intensity could be adjusted to remain constant (70-85% of peak VO2) as the animals improved their running capacity with training. In order to maintain conditions across all four groups, sedentary animals were also placed on treadmills for 1 h/day. The speed of treadmill was constant and set at 2 m/min with no inclination.

4.3 Determination of Glycogen Synthesis/Content

After 8 weeks of diet and exercise interventions, the animals were anesthetized (Ketamine/Xylazine (0.4 mg and 8 mg/100g body weight, respectively) and liver samples were taken. Liver slices weighing ~ 18-20 mg (weight proven to have optimal perfusion based on previous studies in our laboratory) were taken. These slices were incubated at 37°C in Krebs Ringer buffer (KRB) containing BSA (4%), 5.5 mM glucose, and 0.2 μCi/ml D-^{14}C-glucose under either basal or insulin-stimulated (100nM) conditions. The tubes were continuously gasified (95% O_2:5% CO_2) during the for 1 hour. Upon completion of the incubation process, samples were snap frozen in liquid N_2 and then digested in 500 μl of KOH (1M) at 90°C for 30min. Of the digested sample, 100 μl was taken for analysis of glycogen content while the remaining 400 μl was used to assess glycogen synthesis.

For glycogen synthesis, 100 μl of carrier glycogen, 80 μl of Na_2SO_4, and 1.2 ml of cold ethanol were added to the digested solution and left to precipitate overnight. The samples were then centrifuged for 10 min at 13,000 rpm and the supernatant discarded. The remaining pellet was dissolved in 0.5 ml of water and added to 5 ml of scintillation fluid and left to count in the scintillation counter.

Glycogen content measurements were carried out using 100 μl of KOH digested sample. 10% (v/v) of acetic acid 17M, 500 μl of acetate buffer (4.8 pH) with amyloglucosidase (0.5 mg/ml) were added and the resulting solution was left to incubate overnight. On the following day, the solution was neutralized with 1/16 (v/v) of NaOH (5N). Subsequently, 1 ml of ATP-TRA buffer was added to

each sample and then vortexed. Lastly, 1 ml of the solution was placed in a cuvette and counted on the spectrophotometer at 340 nm.

4.4 Insulin Signalling

Slices of liver weighing ~ 18-20 mg were taken and incubated at 37°C for 30 min in KRB containing BSA (4%) and 5.5 mM D-glucose either under basal or insulin-stimulated conditions. The tubes were continuously gasified (95% O_2:5% CO_2) during the incubation period. Following incubation, the samples were then immediately snap frozen in liquid N_2 and stored in -80°C. Insulin signaling was studied using western blotting protocols in which the frozen samples are homogenized in buffer containing 135 mM NaCl, 1 mM $MgCl_2$, 2.7 mM KCl, 20 mM Tris, 1% Triton X-100, 10% Glycerol, protease inhibitor (1:100) (cOmplete ULTRA Tablets), and phosphatase inhibitor (1:100) (PhosStop) (Roche Diagnostics GmbH, Mannheim). Protein concentration was measured using the Bradford method. Finally the samples were diluted 1:1 in lammeli buffer, heated at 95°C for 5min, and subjected to SDS-PAGE. Samples were run against antibodies for PEPCK, PGC-1α, Total AKT, P-AKT (Ser^{473}), Total GSK3α, P-GSK3α, GYS, P-GYS, FAS and β-Actin (loading control). PEPCK antibody was obtained from Abcam (Cambridge, MA). The remaining antibodies were from Cell Signalling Technology Inc (Beverly, MA).

4.5 Determination of Palmitate Oxidation

In order to measure the rate of palmitate oxidation, slices of liver weighing 18-20 g were incubated in KRB at 37°C containing [1-^{14}C] Palmitic acid from GE Healthcare Radiochemicals (Quebec City, QC). One hour later, an eppendorf containing a piece of filter paper covered with 200µl (1:1, vol/vol) 2-phenylethylamine/methanol was added to the vial and the vial was incubated for another hour. At the end of the second hour, 200 µl of sulfuric acid (5N) was added to the incubation medium. Finally, after one-hour incubation, the filter paper was removed, and placed in a scintillation vial for radioactivity counting in 10 ml of scintillation fluid.

4.6 Intraperitoneal Glucose Tolerance Test (IPGTT)

A glucose tolerance test was conducted before and after the diet/exercise interventions. The animals were fasted overnight prior to initiating the procedure. On the day of the test, baseline (Time 0) blood glucose readings were taken from the saphenous vein. Subsequently, rats were injected intraperitoneally (i.p.) with a 20% glucose solution (2 g/kg prepared in physiological saline) and blood samples were taken at 15, 30, 60, and 120 min post injection. Once the test was completed, the rats returned to their regular *ad libitum* diet patterns.

4.7 Intraperitoneal Pyruvate Tolerance Test (IPPTT)

After a 14-hr fast, basal blood glucose was measured from the saphenous vein. Subsequently, a 25% sodium pyruvate solution (2.0 g/kg dissolved in water, pH 7.4) was administered and blood glucose readings were taken at 15, 30, 60, 90, and 120 min post injection. Once the test was completed, the rats returned to their regular *ad libitum* diet patterns.

4.8 Glucose 6-Phopshate (G6P) Quantification

~ 50 mg of liver was homogenized in 150 µl of ice-cold PBS. Samples were centrifuged for 10min @ 12,000rpm (4°C) and the supernatant was extracted. Subsequently, the supernatant was spun down using a 10kDa molecular weight cut off spin column to remove any enzymes, which may interfere with the assay. Hepatic G6P was measured through a calorimetric assay using a commercially available kit (Abcam, Cat # ab83426).

4.9 Triglyceride Quantification

~ 100 mg of liver was heated in 1 ml of 5% NP40 at 90°C for 10min. Samples were homogenized and heated once again at 90°C for 5min. Subsequently, samples were allowed to cool down to room temperature after which they were heated once again for 5min at 90°C. Lastly, they were centrifuged to remove insoluble components and assayed using a commercially available calorimetric kit (Abcam, Cat# ab65336).

4.10 Circulating Insulin

After a 14-hr fast, blood samples were collected from the saphenous vein at week 0, 3, & 6 for analysis of circulating insulin concentrations. Samples were immediately centrifuged @ 13,000 rpm for 10 min (4°C). Plasma was extracted and stored at - 80°C. Plasma was assayed using a commercially available ELISA from EMD Millipore (Cat # EZRMI-13K).

5. Results

5.1 Qualitative Analysis of Hepatic Lipid Accumulation

Qualitative observations of liver samples show successful induction of NAFLD through the diet-induced obesity model. The Sed HF liver (Figure 5B) had severe discolouration compared to controls (Figure 5A). Moreover, a dotted-appearance throughout the HF liver indicates an accumulation of lipid droplets. Exercise attenuated hepatic lipid accumulation in rats on the same HFD (Figure 5C) and presented an appearance that is more similar to the control liver.

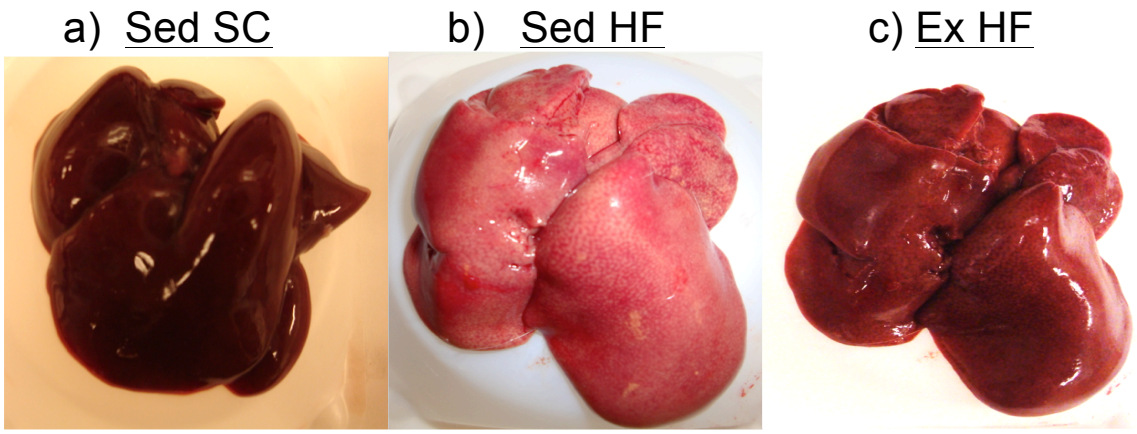

Figure 5. Liver from rats after 8 weeks of chronic diet and/or exercise interventions. A) Sed SC showed excellent perfusion with no signs of lipid accumulation. B) Sed HF had significant lipid accumulation and discolouration. C) Exercise elicits significant improvement in liver appearance even on HFD. Samples were washed in ice-cold PBS.

5.2 Quantitative Analysis of Hepatic Triglyceride Content

Knowing that HFD clearly induced NAFLD, we wanted further to quantify the extent of this hepatic lipid accumulation. We therefore measured hepatic TAG content and as expected, rats on a HFD had significantly higher hepatic lipid accumulation compared to Sed SC. In fact, TAG content was 10.5-fold higher in the Sed HF rats compared to Sed SC. Moreover, Ex HF showed a 24% reduction in hepatic triglyceride content compared to Sed HF animals.

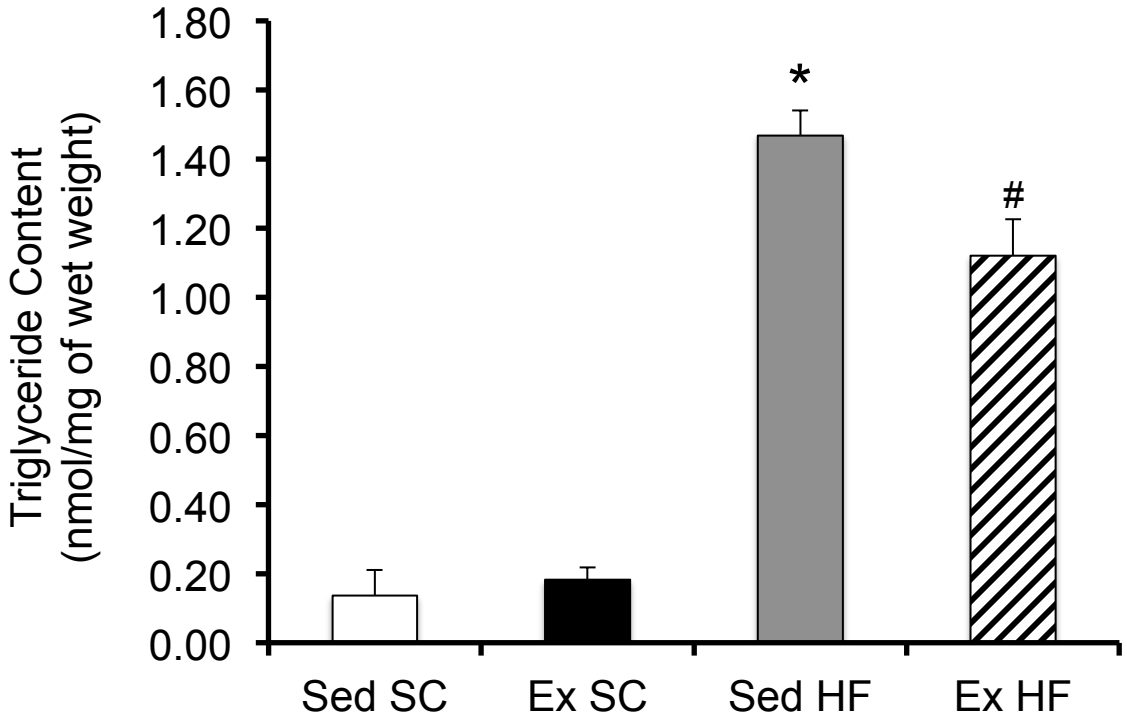

Figure 6. Hepatic triglyceride content. Chronic HF-feeding results in hepatic triglyceride accumulation that is attenuated through exercise. *P<0.05 vs. all other conditions; #P<0.05 vs. Sed HF. Data are expressed as mean ± SEM, n=5. Two-way ANOVA.

5.2 Effects of HFD and Exercise on Circulating Insulin

Circulating insulin was measured throughout the study from blood samples taken at week 0, 3, and 6. Insulin values were similar across all groups at baseline. At week 3, Sed HF rats displayed significantly higher insulin levels, which was heightened further at week 6. Interestingly, exercise reverses insulin resistance even in animals that are fed a HFD.

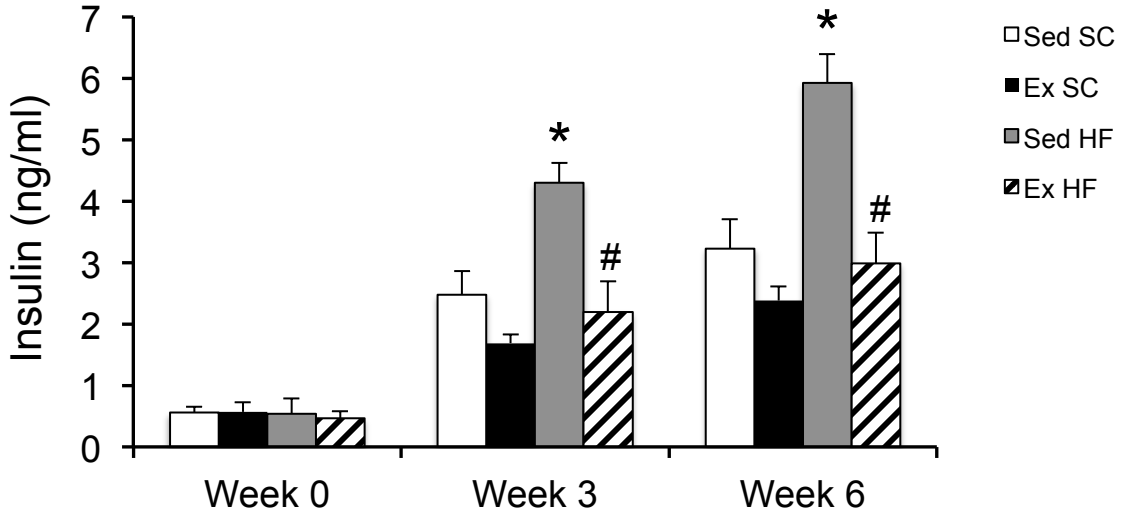

Figure 7 – Indices of whole body insulin-resistance. Blood samples were taken from overnight fasted rats to quantify circulating insulin concentrations in Sed SC, Ex SC, Sed HF, & Ex HF rats. *P<0.05 vs. Sed SC; #P<0.05 vs. Sed HF. Data are expressed as mean ± SEM, n=6. Two-way ANOVA.

5.3 Effects of HFD and Exercise on Whole-Body Glycemic Regulation

In order to examine the effects of HF-feeding and endurance exercise on glucose tolerance we performed an IPGTT (Figure 8A). Sed HF rats displayed significantly higher blood glucose than Sed SC across all time points, including under basal conditions. In fact, the area under the curve (AUC) for glycemia was 1.27-fold higher in Sed HF than Sed SC rats (Figure 8B). Exercise markedly improved blood glucose clearance in both SC- and HF-fed rats by 20% and 13%, respectively. In fact, chronic endurance exercise completely reversed the whole-body insulin resistance found in Sed HF rats. This is supported by the fact that the AUC for glycemia did not differ between Ex HF and Sed SC rats (Figure 8B).

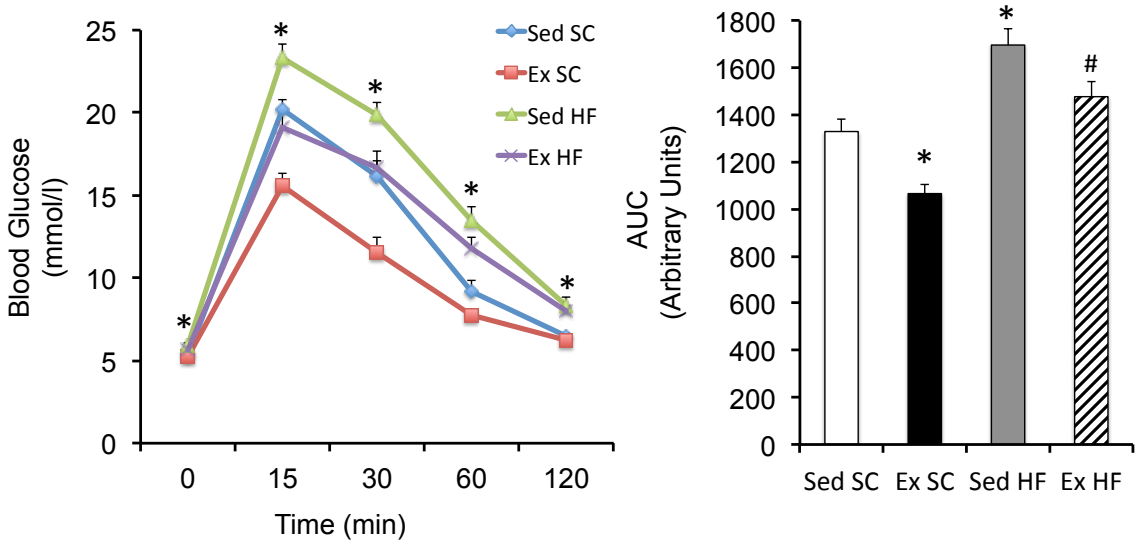

Figure 8. Indices of whole-body Glycemic Control following 8 weeks of HFD and Endurance Training A) IPGTT performed after overnight fasting in Sed SC, Ex SC, Sed HF, Ex HF rats. B) Area under the curve (AUC) corresponding to IPGTT. *P<0.05 vs. Sed SC; #P<0.05 vs. Sed HF. Data are expressed as mean ± SEM, n=18. Two-way ANOVA.

5.4 Pyruvate Tolerance Test

Knowing that HFDs are associated with elevated plasma glucose and impaired glucose clearance, we wanted to understand whether this outcome of insulin resistance could be attributed particularly to the liver. As a result, we performed a pyruvate tolerance test to identify liver-specific insulin resistance and uncontrolled glucose production. Preliminary studies analyzing the effects of HFD on pyruvate tolerance show significantly higher blood glucose concentrations at 30, 60, 90, and 120min post injection (Figure 9A). Moreover, HFD elicits significantly higher glucose production with significance using area under the curve (1137.4 vs. 1496.6 Arbitrary Units) (Figure 9B).

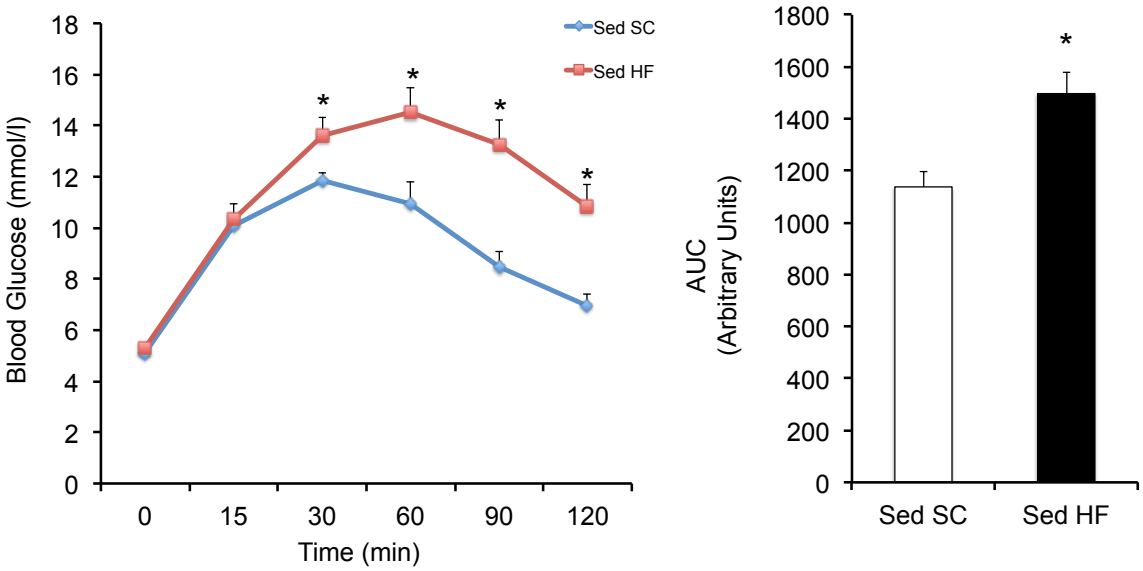

Figure 9. Indices of liver-specific insulin resistance and pyruvate intolerance following 8 weeks of HFD. A) IPPTT performed after overnight fasting in Sed SC and Sed HF rats. B) Area under the curve (AUC) corresponding to IPPTT. *P<0.05 vs. Sed SC. Data are expressed as mean ± SEM, n=10. Independent *t*-Test.

5.5 Glycogen Synthesis

Given the elevated hepatic glucose production, and whole body as well as liver-specific insulin resistance seen following chronic HFD, it was imperative to understand how hepatic glycogen synthesis operates under these conditions. We therefore incubated slices of liver under basal and insulin-stimulated conditions and quantified the rate of glycogen synthesis. Exercise reduced the rate of glycogen synthesis in both basal and insulin stimulated livers. The exercise-induced differences in glycogen synthesis were only significant in HF animals under basal conditions, although SC exercisers still saw ~ 20% reduction (Figure 10A). Furthermore, upon insulin stimulation, both SC and HF exercisers saw significant reduction in the rate of glycogen synthesis (Figure 10B).

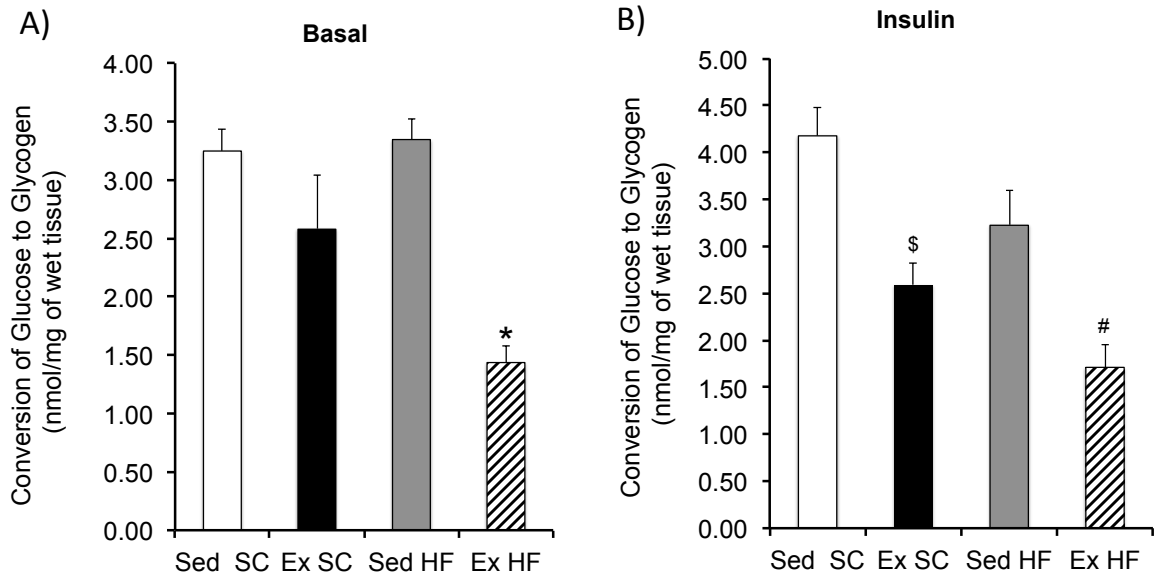

Figure 10. Effects of SC- or HF-feeding and exercise on rates of glycogen synthesis. A) Comparing Sed SC, Ex SC, Sed HF, & Ex HF under basal conditions. B) Comparing Sed SC, Ex SC, Sed HF, & Ex HF under insulin stimulated (100 nM) conditions. Slices of liver were incubated for 1 hour in KRB buffer in the presence or absence of insulin (100nM) and radiolabelled D-^{14}C-glucose. All values are expressed as nmol/mg of wet tissue. *P<0.05 vs. all other conditions. $^{\$}$P<0.05 vs. Sed SC. $^{\#}$P<0.05 vs. Sed HF. Data are expressed as mean ± SEM, n=6. Two-way ANOVA.

5.6 Glycogen Content

Knowing that exercise reduced the conversion of glucose to glycogen, we wanted to know whether this reduction translated into a reduction in overall glycogen content. As a result we used a sample from the same incubated liver slices used in the glycogen synthesis assay to quantify glycogen content. We found no effect of insulin stimulation on absolute glycogen content levels. Moreover, there were no differences with diet or training.

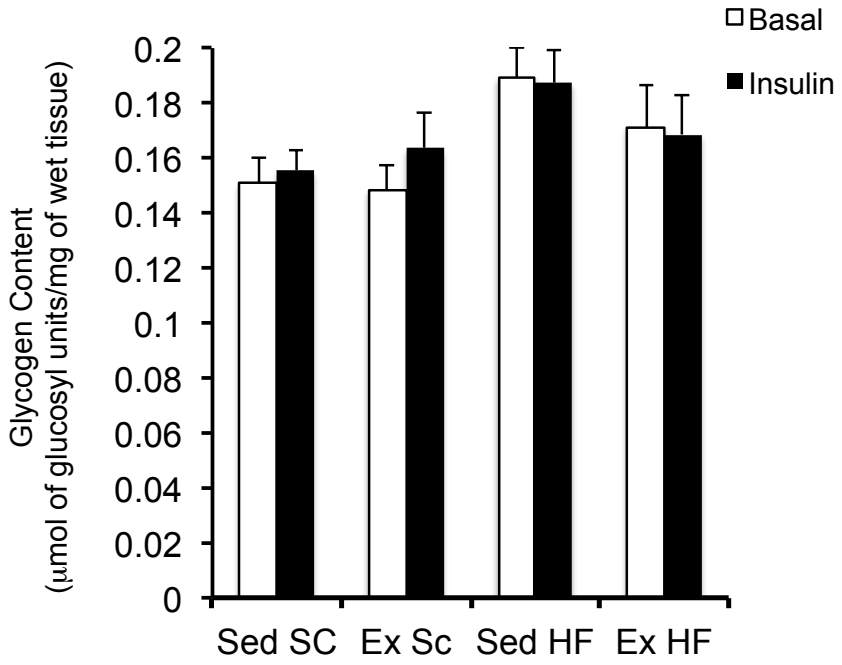

Figure 11. Effects of diet and exercise on glycogen content in Sed SC, Ex SC, Sed HF, and Ex HF rats under basal and insulin-stimulated conditions. Slices of liver were incubated for 1 hour in KRB buffer either in the absence or presence of insulin (100 nM). All values are expressed as μmol of glucosyl units/mg of wet tissue. Data are expressed as mean ± SEM, n=9. Two-way ANOVA.

5.7 Glucose 6-Phosphate

In order to better understand the mechanism behind reduced rates of glycogen synthesis in exercised animals, we measured intracellular G6P. We assessed G6P hypothesizing that exercised animals may have reduced G6P resulting in a blunted allosteric activation of GYS. Contrary to our expectations, a mild increase was seen in exercised animals although these observations were not found to be significantly different.

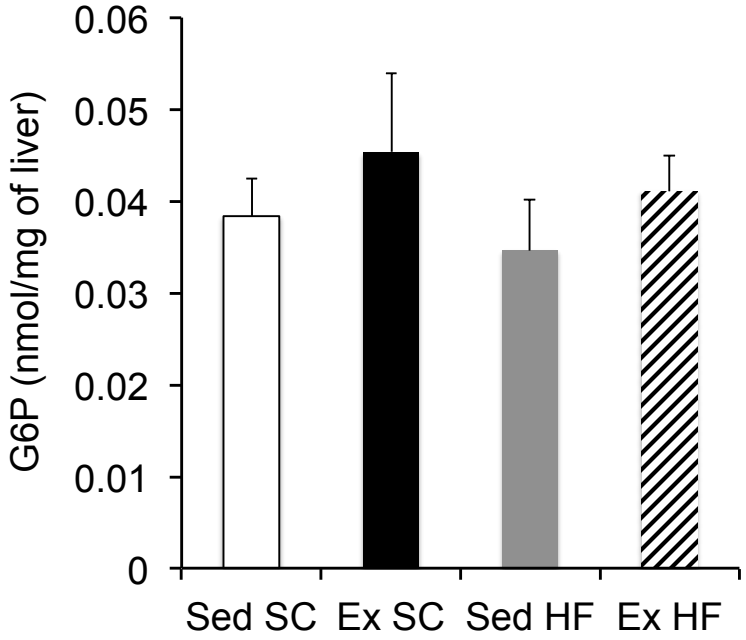

Figure 12. Measurement of G6P using calorimetric assay. Comparing Sed SC, Ex SC, Sed HF, and Ex HF liver homogenates under basal conditions. No Significant differences were found between groups. Data are expressed as mean ± SEM, n=6. Two-way ANOVA.

5.8 Effects of HFD and Exercise on Insulin Signalling for Glycogen Synthesis

We performed western blot analysis in order to determine the effects of HFD and exercise on intracellular proteins involved in the insulin-signaling cascade for glycogen synthesis. Samples were run against antibodies for phosphorylated forms of AKT, GSK3, and GYS. AKT phosphorylation was significantly greater at Ser^{473} with chronic exercise under both diets (Figure 13A). GSK3α, the downstream protein from AKT saw increased phosphorylation of its α isoform at Ser^{21} with exercise, although this difference was only found to be significant in the Ex SC group (Figure 13B). Finally, despite increased phosphorylation of AKT and GSK3α in exercised animals, GYS, which is negatively regulated by phosphorylation remained phosphorylated at Ser^{641} with exercise; a result that was significant in Ex HF animals (Figure 13C). Nevertheless, western blots for phosphorylation of GYS support earlier data depicting reduced rates of glycogen synthesis in exercised rats.

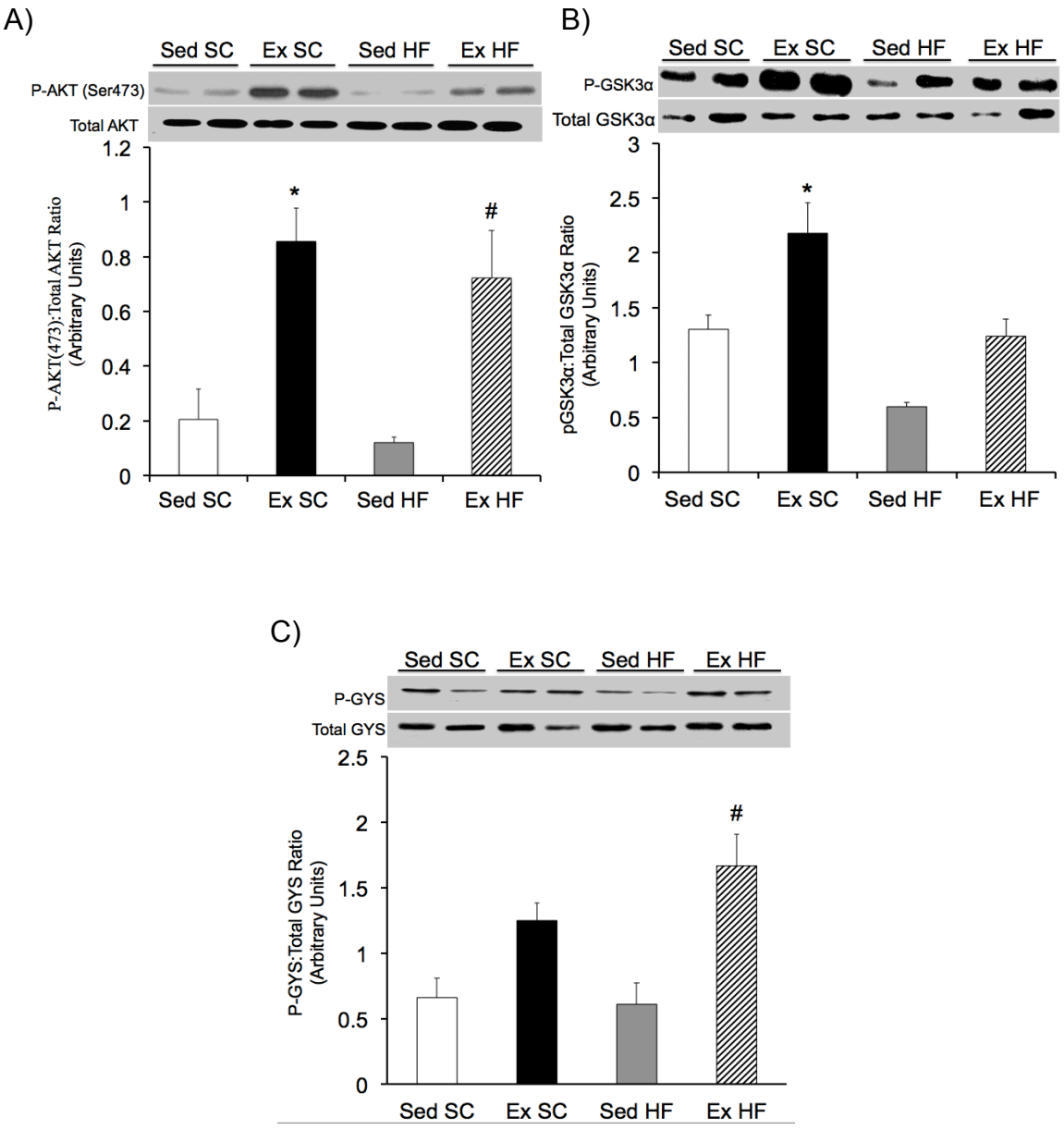

Figure 13. Representative blots and densitometric analysis of proteins in the insulin-signaling cascade for glycogen synthesis. Effects of diet and exercise on phosphorylation of a) AKT (n=5), b) GSK3α (n=6), and c) GYS (n=5) in frozen liver homogenates. Samples were prepared for SDS-Page as described in methods. $^{*}P<0.05$ vs. Sed SC. $^{\#}P<0.05$ vs. Sed HF. Data are expressed as mean ± SEM. Two-way ANOVA.

5.9 Effect of HFD & Exercise on Proteins involved in Gluconeogenesis

Having witnessed the elevated GNG in response to HFD through the pyruvate tolerance test, we subsequently performed western blots for proteins involved in the GNG pathway. HFD significantly increased cytosolic PEPCK (Figure 14A). However, when fed a HFD in conjunction with exercise, these HF-induced elevations in PEPCK were significantly reduced. The reduction in PEPCK with exercise is accompanied by paralleled reductions in PGC-1α (Figure 14B).

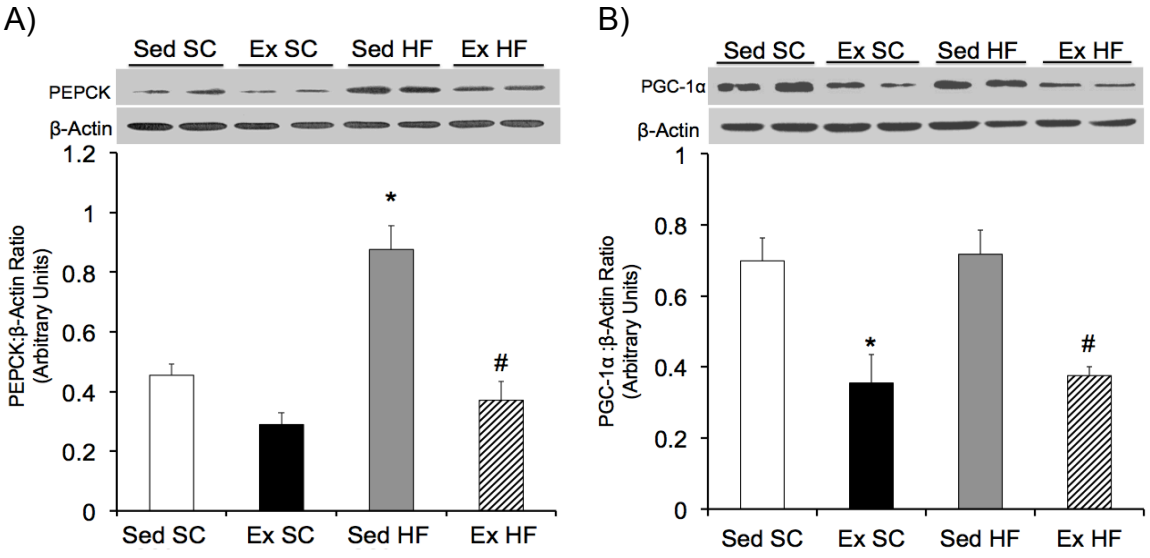

Figure 14. Representative blots and densitometric analysis of gluconeogenic proteins. Western Blots were performed for a) PEPCK (n=5) and b) PGC-1α (n=4) in frozen liver homogenates. Samples were prepared for SDS-Page as described in methods. $^{*}P<0.05$ vs. Sed SC. $^{\#}P<0.05$ versus Sed HF. Data are expressed as mean ± SEM. Two-way ANOVA.

5.10 Effects of HFD & Exercise on *de novo* Lipogenesis

Additional western blots were performed for FAS, the terminal protein in *de novo* lipid synthesis. HFD results in significantly lower FAS content. Moreover, exercise had no effect on the content of this protein.

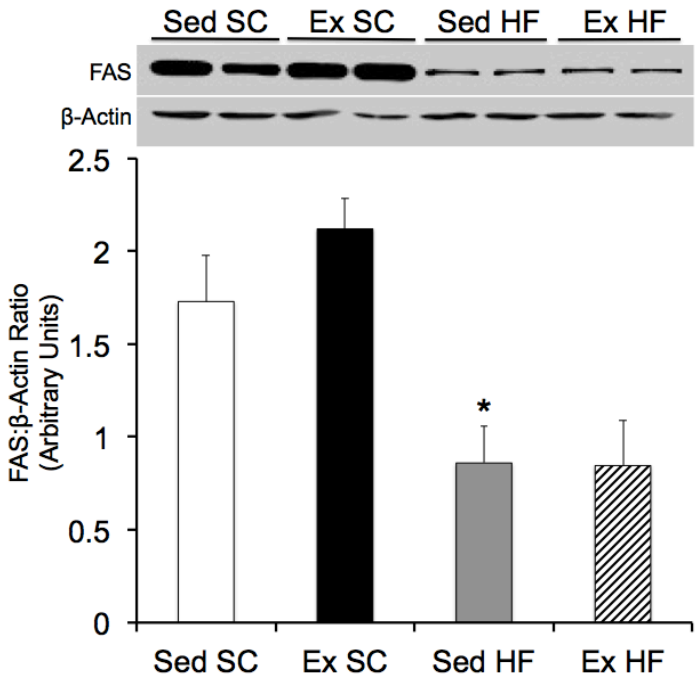

Figure 15. Representative blots and densitometric analysis of FAS. Western Blots were performed for FAS in frozen liver homogenates. Samples were prepared for SDS-Page as described in methods. $^{*}P<0.05$ vs. Sed SC. Data are expressed as mean ± SEM, n=5. Two-way ANOVA.

5.11 Palmitate Oxidation

We measured palmitate oxidation to understand how HFD and exercise affects rates of FAO in the liver. As expected, HFD increased hepatic FAO although this was not found to be significant. Given that qualitative observations indicated a reversal of NAFLD, we expected to see higher rates of palmitate oxidation upon exercise. In contrast to our expectations, exercise reduced oxidation; a result that was found to be significant in the Ex HF group.

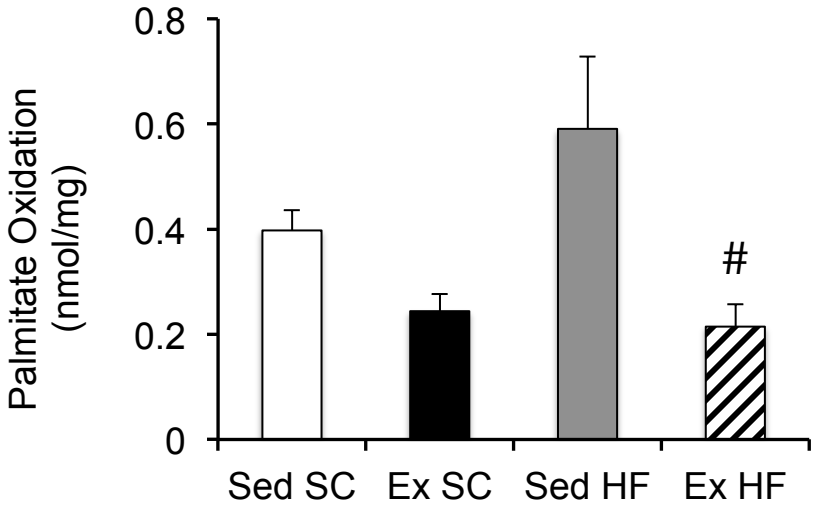

Figure 16. Measures of palmitate oxidation under basal conditions Liver slices were incubated in [1-^{14}C] Palmitic acid at 37°C. One hour later, an eppendorf containing a piece of filter paper covered with phenetylamine (200 μl of a 1:1 dilution in methanol) was added to the vial and the vial was incubated for another hour. At the end of the second hour, 200 μl of sulfuric acid (5N) was added to the incubation medium. Finally, after one-hour incubation, the filter paper was removed, and placed in a scintillation vial for radioactivity counting in 10 ml of scintillation fluid. $^{\#}P<0.05$ versus Sed HF. Data are expressed as mean ± SEM, n=5. Two-way ANOVA.

5.12 Effect of HFD & Exercise on Subcutaneous WAT Cell Lipolysis

In order to test the contribution of lipolysis to NAFLD, we measured free glycerol in subcutaneous WAT cells. HFD elevated lipolysis significantly when compared to standard chow controls. Moreover, feeding a HFD with chronic endurance training significantly reduces lipolysis by ~ 57% compared to the Sed HF group. These results are in line with the qualitative observations of hepatic fat content in addition to hepatic triglyceride results alluded to in Figure 1 and 2 respectively.

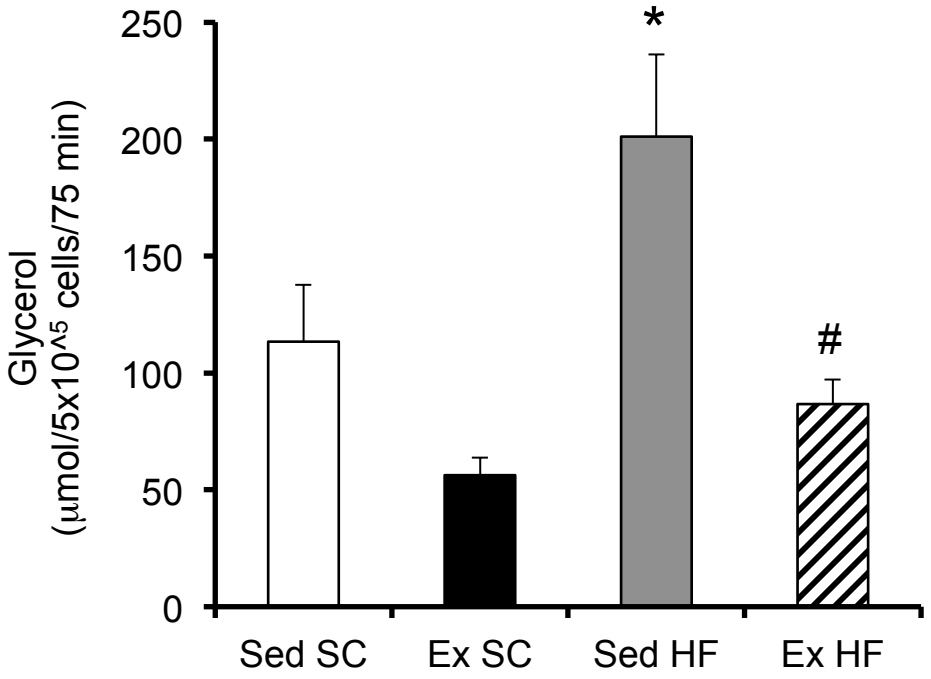

Figure 17. Measures of WAT cell lipolysis under basal conditions. WAT cells were isolated and lipolysis was measured in Sed SC, Ex SC, Sed HF, and Ex HF rats . *P<0.05 versus Sed SC. #P<0.05 versus Sed HF. Data are expressed as mean ± SEM, n=6. Two-way ANOVA.

6. Discussion

Here we report that chronic endurance training exerts an anti-steatotic effect and improves insulin signaling in the liver of HF-fed rats. This is shown through visual observations (Figure 5B) in which we spotted severe discolouration in liver from HF-fed rats. Moreover, a dotted appearance throughout the course of the liver indicates excessive hepatic lipid accumulation. In line with these observations, we have evidence to show HFD induces a 10.5-fold greater hepatic triglyceride content compared to those fed a SC diet (Figure 6). Importantly, exercise reduced the hepatic TG content by 24%. These observations are indicative of a successful induction of NAFLD using our diet-induced obesity model and that exercise can significantly reduce HFD-induced hepatic lipid accumulation.

It has been reported that the body is able to preferentially shift substrate metabolism to the most abundant and readily available substrate (42). As such, it would be expected that under conditions of HF-feeding, the system would preferentially oxidize fats in an attempt to remove them and prevent ectopic lipid accumulation. Such is the case in the rats of this study, as HF-feeding has shown to increase the rate of palmitate oxidation by 1.48-fold compared to SC rats (Figure 16). However, this compensatory mechanism seems to be overpowered by the abundance of incoming dietary lipids, as well as by the enhanced supply of NEFAs through increased white adipose tissue lipolysis. Consequently, ectopic fat accumulation continues to take place despite having elevated lipid oxidation in the liver. These results are consistent with findings by Bugianesi et al, who found

that increased hepatic lipid infiltration was accompanied by elevated lipid oxidation in non-diabetic NAFLD patients (9).

Numerous studies have supported the notion that NAFLD is in part induced through increased *de novo* lipogenesis (10, 76). We provide evidence to suggest otherwise. Under resting conditions, western blot analysis revealed that FAS, the terminal enzyme of *de novo* lipid synthesis, was significantly reduced with HF-feeding (Figure 15). As a result, *de novo* lipogenesis is expected to be reduced. This anabolic process is normally activated under conditions of elevated insulin and low glucagon levels. However, in HF steatotic animals, insulin signaling is impaired (77), which should cause a decline intracellular malonyl-CoA levels. As a result, there would be an increase in CPT1 activity and FAO, while simultaneously reducing *de novo* lipid synthesis. Shimomura et al., found that despite a reduction in IRS2 content and phosphorylation of AKT, SREBP-1c mRNA increased as a consequence of obesity-induced hyperinsulinemia. Accordingly, they suggest that there must be an alternate pathway independent of IRS2 to elicit these insulin-mediated effects (78). However, due to post-translational modifications, the presence of mRNA doesn't always guarantee the presence or activity of protein. We were able to show FAS protein content, which is normally elevated in an SREBP-1c induced manner, is in fact reduced with HFD.

Lastly, enhanced lipolysis is believed to be a major source of NEFA delivery to the liver in an insulin resistant state (Figure 7). Measurement of lipolysis in subcutaneous WAT cells revealed significantly higher (1.77-fold) levels of free glycerol (a marker of lipolysis) following high fat feeding (Figure 17).

Chronic endurance training reduced basal lipolysis by ~ 57% in the subcutaneous inguinal fat, an effect that likely resulted from exercise-induced improvement in insulin sensitivity. We therefore conclude that the majority of lipid abundance seen in NAFLD patients is due to excessive fat intake through the diet and increased lipolysis resulting from insulin resistance, but not due to elevated *de novo* lipogenesis.

Interestingly, despite the clearance of lipids from the liver following chronic exercise, hepatic lipid oxidation is reduced in all exercised rats (Figure 16). This reduction was found to be significant in Ex HF animals compared to the Sed HF group. Despite the preferential shift to fat oxidation under basal conditions in a trained state (79, 80), hepatic lipid oxidation itself seems to react differently. Considering fatty acid oxidation occurs in the mitochondria, and PGC-1α regulates mitochondrial biogenesis, the significant reduction in PGC-1α content (Figure 14B) following training may explain the reduced intrahepatic fat oxidation. These results suggest that although hepatic lipid content is reduced with exercise, these lipids are not being heavily oxidized in the liver, but rather in peripheral tissues such as skeletal muscle which have their metabolic activity highly increased during chronic exercise (81).

It has been well established in the literature that NAFLD is closely associated with T2D, and thus impaired glucose regulation. We therefore shifted our attention to how the system goes about maintaining glycemic control under these conditions. Clearly high fat diet induces severe hyperinsulinemia which progressively worsens with chronic HFD (Figure 7). Results from an IPGTT (Figure 8) are in agreement with previous studies which show significant glucose

intolerance and insulin resistance following HFD (82, 83). In fact, these rats display significantly higher blood glucose readings across all time points including basal glucose readings compared to Sed SC (control). This may be attributed to the disruption of a number of glucose homeostatic mechanisms including GNG, glycogen synthesis, glycolysis, and glycogenolysis. Moreover, an IPGTT assesses whole body glucose intolerance and IR; therefore, the resulting hyperglycemia may also be attributable to metabolic disruptions that HF-feeding caused in peripheral tissues such as skeletal muscle or adipose tissue. Although the exact mechanism behind this insulin resistance is unclear, we provide evidence that hepatic lipid accumulation is the culprit behind this impairment. Our reasoning for this lies behind the fact that following 8 weeks of chronic exercise, NAFLD is significantly reduced (Figure 5C & Figure 6) and glucose tolerance was improved in exercised animals fed either standard chow or a HFD (Figure 8B). These data suggest that exercise is an effective therapeutic tool in reducing whole-body glucose intolerance and insulin resistance.

In both diabetes and obesity-induced insulin resistance, hepatic glucose production is a significant contributor to both the elevated fasting hyperglycemia and uncontrolled postprandial hyperglycemia. Although numerous IPGTT measures in our lab were indicative of whole body insulin resistance, we wanted to be able to demonstrate that this whole body glucose intolerance was in part attributable to hepatic insulin resistance. We therefore conducted an IPPTT in our preliminary studies involving control and HF rats to establish this. As shown in Figure 9A, the HF animals convert a larger proportion of the injected pyruvate into glucose and releases it into circulation. As a result, they display significantly

higher plasma glucose levels (Figure 9B). A higher rate of conversion of GNG precursors to glucose is indicative of insulin resistance and thus overactive GNG. Therefore, in patients with NAFLD, elevated GNG is one of the culprits contributing to elevated fasting and postprandial hyperglycemia in diabetes and NAFLD.

To further investigate the mechanisms behind elevated *de novo* glucose production, we performed western blot analysis of key proteins involved in the GNG pathway. As expected, HF-feeding resulted in significantly higher PEPCK content, which would promote the GNG pathway illustrated through the IPPTT. Interestingly, and in agreement with current literature, both PEPCK and PGC-1α parallel one another in their expression patterns (31, 33). That is, with chronic exercise (a more insulin sensitive system), both PGC-1α and PEPCK content are reduced (Figure 14). Given that PGC-1α is a transcriptional co-activator of GNG genes, these results suggest that reduced PGC-1α results in less transcription of PEPCK. The result is reduced *de novo* glucose production and improved blood glucose profiles in exercised animals. Moreover, the activity of PGC-1α depends highly on transcription factor availability (28, 33). Normally, FOXO1 is excluded from the nucleus through AKT mediated phosphorylation, thereby preventing PGC-1α-FOXO1 interaction and gene transcription (40). Once again, with exercise, we demonstrate improved insulin sensitivity through increased AKT phosphorylation in both standard chow and HF fed rats (Figure 13A). As a result, this would promote FOXO1 phosphorylation and exclusion from the nucleus, thereby reducing GNG gene transcription. These results are consistent with findings from Ropelle et al. who observed similar AKT mediated reduction in

PGC-1α and a concomitant reduction in GNG genes in rats subjected to two 3h acute exercise bouts (40). From this it is clear that the exercise-induced reduction in GNG is not only present after acute exercise, but also during resting conditions following chronic endurance training.

Although we have shown that hyperglycemia in NAFLD is in part due to elevated GNG, one cannot ignore the contribution of glycogen synthesis. Aside from glycolysis, glycogen synthesis is a significant contributor to the clearance of circulating glucose. Here we provide novel evidence to suggest that following chronic endurance training, rates of hepatic glycogen synthesis are not increased, but rather reduced in basal and insulin-stimulated liver slices (Figure 10). This presents a paradoxical finding that led us to ask the following question: how can hepatic glycogen synthesis be blunted in exercised animals when a number of metabolic factors support a more insulin sensitive system with exercise? Despite improved AKT and GSK3α signaling, hepatic glycogen synthesis was reduced with exercise (Figure 13). However, this impairment of glycogen synthesis is clearly not due to an insulin resistant state. The reduction in glycogen synthesis is further supported by increased phosphorylation of GYS in exercised animals. To further investigate this seemingly counterintuitive mechanism, we measured hepatic G6P (Figure 12) to gain insight into whether there was less allosteric activation of GYS with exercise. No significant differences were found with exercise. In fact a mild increase in G6P was found in trained animals, which would theoretically promote allosteric activation of GYS in contrast to our observations. Nevertheless, there is a sufficient amount of G6P available to allosterically activate glycogen synthesis. Therefore, there must be

some alternate metabolic fate of glucose or increasing energy demands in peripheral tissues, which force the liver to export glucose rather than storing it.

Having identified blunted glycogen synthesis in both basal and insulin stimulated conditions, we then measured glycogen content (Figure 11) from the same liver slices used to measure glycogen synthesis. Although the rate of conversion of glucose to glycogen was reduced with exercise, this did not compromise total glycogen content. No differences in were found within groups with insulin stimulation or between groups with basal or insulin-stimulation.

Impaired glycogen synthesis would normally suggest elevated plasma glucose and resultant hyperglycemia. Remarkably, this is not the case as we clearly demonstrate significant improvements in both glucose tolerance and markers of *de novo* glucose production with exercise. These results suggest an alternate metabolic fate of glucose following chronic endurance training. It could be that despite having reduced *de novo* glucose production, hepatic glucose output increases (as a result of increased glycogenolysis) in an attempt to meet the heightened energy demands in a trained system.

7. Conclusion

Based on our findings it is clear that chronic HF-feeding induces hepatic steatosis to an extent that compromise hepatic as well as whole-body glucose metabolism. Despite a compensatory increase in the rate of palmitate oxidation, the system is unable to clear the excessive fats incoming through both the diet and to a smaller extent, ongoing lipolysis. We have shown that exercise can be used as a therapeutic approach to treat the metabolic abnormalities of NAFLD to an extent that significantly improves insulin sensitivity, glucose tolerance, and *de novo* glucose production.

Insulin resistance is clearly reduced with exercise as illustrated by measures of circulating insulin and a smaller IPGTT AUC in both standard chow and high fed rats. Moreover, phosphorylation of key proteins involved in insulin signaling, namely AKT(Ser^{473}) and GSK3α are enhanced with training. When studying GNG, both PEPCK and PGC-1α are significantly reduced with training. These effects are likely due to improved insulin sensitivity in the absence of hepatic lipotoxicity.

Here, we present the novel findings of the reduced rate of glycogen synthesis following chronic endurance training. To our knowledge, we are the first to witness such a response with chronic HF-feeding and exercise even under insulin-stimulated conditions. Importantly, these observations were 48h after the last bout of endurance training, indicating that any findings are a result of chronic rather than acute exercise. As a result, in a trained system the reversal of NAFLD seems to be associated with a preferential shift in substrate metabolism that enhances whole-body glucose and hepatic lipid clearance.

8. Future Directions

In our study we observed that chronic endurance exercise has the capacity to attenuate HFD induced NAFLD. We also detected paralleled reductions in whole body glucose intolerance and improvements in insulin sensitivity. These observations are seen even in the paradoxical conditions of both reduced hepatic palmitate oxidation and glycogen synthesis in rats under chronic HF-feeding and endurance training. Accordingly, there are a number of follow-up experiments to be conducted that may potentially clarify the mechanism behind these findings.

8.1. Hepatic glucose output

Perhaps the reduction in glycogen synthesis is in part due to increased hepatic glucose output in a trained system. This may be a valid mechanism considering the role of the liver is to export glucose to peripheral tissues based on energy demands of the body. Increasing energy demands in trained animals would require the liver to release glucose through glycogenolysis into circulation rather than storing it as glycogen. These experiments can be carried out by incubating liver slices in KRB buffer in the absence of glucose and subsequently measuring glucose in the buffer. Moreover, three slices of liver will be taken for basal, insulin, and glucagon stimulated measures. Due to the absence of glucose in the buffer, glucose present after the incubation period must therefore be a result of HGO.

8.2. Glucose oxidation

Given that hepatic glycogen synthesis is reduced following training, this raises the possibility of heightened glucose demand in peripheral tissues. Accordingly, measuring both hepatic as well as whole-body glucose oxidation may help clarify the fate of glucose in exercised animals.

8.3 Western Blot analysis of ACC & Regulators of Glycogen Synthase

In order to explain the reduction in palmitate oxidation in the liver, it is imperative that we measure both total and phosphorylated ACC. Reduced phosphorylation of ACC with exercise is expected given that this protein is active in its dephosphorylated state. Active ACC results in increased production malonyl-CoA, however we have reported in the present study that FAS activity is reduced with high fat diet. Accordingly, a build up of malonyl-CoA would in theory inhibit fatty acid oxidation (as we have shown).

Next, we found no differences with respect to intra-hepatic G6P concentrations between any of the groups. Therefore, it is unlikely that the inactivation of GYS seen with training is accomplished through allosteric regulation. Therefore, we need to focus our attention on known covalent modifiers of GYS activity. These include AMPK, PKA, and PP1.

9. References

1. Sturm R, Ph D, Economist S. Morbid Obesity Rates Continue to Rise Rapidly in the US. *Int J Obes* 2013;37:889–891.

2. Lobstein T, Baur L, Uauy R. Obesity in children and young people : a crisis in public health. *IASO Int Obes TaskForce* 2004;5 (1):4–85.

3. Tremblay MS, Warburton DER, Janssen I, *et al.* New Canadian physical activity guidelines. *Appl Physiol Nutr Metab* 2011;36:36–46; 47–58.

4. Finucane MM, Stevens GA, Cowan MJ, *et al.* National, regional, and global trends in body-mass index since 1980: Systematic analysis of health examination surveys and epidemiological studies with 960 country-years and 9??1 million participants. *Lancet* 2011;377:557–567.

5. Conlon B a, Beasley JM, Aebersold K, Jhangiani SS, Wylie-Rosett J. Nutritional management of insulin resistance in nonalcoholic fatty liver disease (NAFLD). *Nutrients* 2013;5:4093–114.

6. Parekh S, Anania F a. Abnormal Lipid and Glucose Metabolism in Obesity: Implications for Nonalcoholic Fatty Liver Disease. *Gastroenterology* 2007;132:2191–2207.

7. Kelley DE, McKolanis TM, Hegazi R a F, Kuller LH, Kalhan SC. Fatty liver in type 2 diabetes mellitus: relation to regional adiposity, fatty acids, and insulin resistance. *Am J Physiol Endocrinol Metab* 2003;285:E906–E916.

8. Marchesini G, Brizi M, Bianchi G, *et al.* Nonalcoholic Fatty Liver Disease. *Diabetes* 2001;50:1844–1850.

9. Bugianesi E, Gastaldelli a., Vanni E, *et al.* Insulin resistance in non-diabetic patients with non-alcoholic fatty liver disease: Sites and mechanisms. *Diabetologia* 2005;48:634–642.

10. Lambert JE, Ramos-Roman MA, Browning JD, Parks EJ. Increased de novo lipogenesis is a distinct characteristic of individuals with nonalcoholic fatty liver disease. *Gastroenterology* 2014;146:726–735.

11. Takuma Y, Nouso K. Nonalcoholic steatohepatitis-associated hepatocellular carcinoma: our case series and literature review. *World J Gastroenterol* 2010;16:1436–1441.

12. Cintra DE, Ropelle ER, Vitto MF, *et al.* Reversion of hepatic steatosis by exercise training in obese mice: The role of sterol regulatory element-binding protein-1c. *Life Sci* 2012;91:395–401.

13. Bacchi E, Negri C, Targher G, *et al.* Both resistance training and aerobic training reduce hepatic fat content in type 2 diabetic subjects with nonalcoholic fatty liver disease (the RAED2 Randomized Trial). *Hepatology* 2013;58:1287–1295.

14. Sherwin RS. Role of the liver in glucose homeostasis. *Diabetes Care* 1980;3:261–265.

15. Saltiel AR, Kahn CR. Insulin signalling and the regulation of glucose and lipid metabolism. *Nature* 2001;414:799–806.

16. Berridge MJ. Cell Signalling Biology: Module 2 - Cell signalling pathways. *Biochem J* 2012:1–130.

17. Cross D a, Alessi DR, Cohen P, Andjelkovich M, Hemmings B a. Inhibition of glycogen synthase kinase-3 by insulin mediated by protein kinase B. *Nature* 1995;378:785–9.

18. MacAulay K, Doble BW, Patel S, *et al.* Glycogen synthase kinase 3alpha-specific regulation of murine hepatic glycogen metabolism. *Cell Metab* 2007;6:329–337.

19. Von Wilamowitz-Moellendorff A, Hunter RW, García-Rocha M, *et al.* Glucose-6-phosphate-mediated activation of liver glycogen synthase plays a key role in hepatic glycogen synthesis. *Diabetes* 2013;62:4070–4082.

20. Lavoie L, Dimitrakoudis D, Marette A, *et al.* Opposite effects of hyperglycemia and insulin deficiency on liver glycogen synthase phosphatase activity in the diabetic rat. *Diabetes* 1993;42:363–366.

21. Nielsen JN, Richter E a. Regulation of glycogen synthase in skeletal muscle during exercise. *Acta Physiol Scand* 2003;178:309–319.

22. O'Doherty RM, Lehman DL, Télémaque-Potts S, Newgard CB. Metabolic impact of glucokinase overexpression in liver: Lowering of blood glucose in fed rats is accompanied by hyperlipidemia. *Diabetes* 1999;48:2022–2027.

23. Misra P, Chakrabarti R. The role of AMP kinase in diabetes. *Indian J Med Res* 2007;125:389–398.

24. Bultot L, Guigas B, Von Wilamowitz-Moellendorff A, *et al.* AMP-activated protein kinase phosphorylates and inactivates liver glycogen synthase. *Biochem J* 2012;443:193–203.

25. Ros S, Zafra D, Valles-Ortega J, *et al.* Hepatic overexpression of a constitutively active form of liver glycogen synthase improves glucose homeostasis. *J Biol Chem* 2010;285:37170–37177.

26. Berridge MJ. Cell Signalling Biology: Module 7 - Cellular Processes. *Biochem J* 2012:1–136.

27. Brady MJ, Saltiel a R. The role of protein phosphatase-1 in insulin action. *Recent Prog Horm Res* 2001;56:157–173.

28. Rhee J, Inoue Y, Yoon JC, *et al.* Regulation of hepatic fasting response by PPARgamma coactivator-1alpha (PGC-1): requirement for hepatocyte nuclear factor 4alpha in gluconeogenesis. *Proc Natl Acad Sci U S A* 2003;100:4012–4017.

29. Aharoni-Simon M, Hann-Obercyger M, Pen S, Madar Z, Tirosh O. Fatty liver is associated with impaired activity of PPARγ-coactivator 1α (PGC1α) and mitochondrial biogenesis in mice. *Lab Invest* 2011;91:1018–1028.

30. Wu M V., Bikopoulos G, Hung S, Ceddia RB. Thermogenic Capacity Is Antagonistically Regulated in Classical Brown and White Subcutaneous Fat Depots by High Fat Diet and Endurance Training in Rats. *J Biol Chem* 2014;289:34129–34140.

31. Yoon JC, Puigserver P, Chen G, *et al.* Control of hepatic gluconeogenesis through the transcriptional coactivator PGC-1. *Nature* 2001;413:131–138.

32. Besseiche a., Riveline J-P, Gautier J-F, Bréant B, Blondeau B. Metabolic roles of PGC-1α and its implications for type 2 diabetes. *Diabetes Metab* 2015:1–11.

33. Puigserver P, Rhee J, Donovan J, Kitamura Y, Altomonte J, Dong H. Insulin-regulated hepatic gluconeogenesis through FOXO1 – PGC-1 a interaction. *Nature* 2003;423:550–555.

34. Matsumoto M, Pocai A, Rossetti L, DePinho R a., Accili D. Impaired Regulation of Hepatic Glucose Production in Mice Lacking the Forkhead Transcription Factor Foxo1 in Liver. *Cell Metab* 2007;6:208–216.

35. Yoon JC, Puigserver P, Chen G, *et al.* Control of hepatic gluconeogenesis through the transcriptional coactivator PGC-1. *Nature* 2001;413:131–138.

36. Gómez-Ambrosi J, Frühbeck G, Alfredo Martínez J. Rapid in vivo PGC-1 mRNA upregulation in brown adipose tissue of Wistar rats by a β3-adrenergic agonist and lack of effect of leptin. *Mol Cell Endocrinol* 2001;176:85–90.

37. Hanson RW. A Perspective on the Biology of Phosphoenolpyruvate Carboxykinase 55 Years After Its Discovery. *Am Soc Biochem Mol Biol* 2009:1–6.

38. Hakimi P, Johnson MT, Yang J, *et al.* Phosphoenolpyruvate carboxykinase and the critical role of cataplerosis in the control of hepatic metabolism. *Nutr Metab (Lond)* 2005;2:33.

39. Yang J, Kalhan SC, Hanson RW. What is the metabolic role of phosphoenolpyruvate carboxykinase? *J Biol Chem* 2009;284:27025–27029.

40. Ropelle ER, Pauli JR, Cintra DE, *et al.* Acute exercise modulates the Foxo1/PGC-1alpha pathway in the liver of diet-induced obesity rats. *J Physiol* 2009;587:2069–2076.

41. George F CJ, Ashmore J, Renold AE, A.Baird H. Review Blood Glucose and the Liver *. *Am J Med* 1959;26:264–282.

42. Randle PJ, Garland PB, Hales CN, Newsholme E a. The glucose fatty-acid cycle. Its role in insulin sensitivity and the metabolic disturbances of diabetes mellitus. *Lancet* 1963;1:785–789.

43. Mabrouk GM, Helmy IM, Thampy KG, Wakil SJ. Acute hormonal control of acetyl-CoA carboxylase. The roles of insulin, glucagon, and epinephrine. *J Biol Chem* 1990;265:6330–6338.

44. Wakil SJ, Abu-Elheiga L a. Fatty acid metabolism: target for metabolic syndrome. *J Lipid Res* 2009;50 Suppl:S138–S143.

45. McGarry JD. Banting lecture 2001: dysregulation of fatty acid metabolism in the etiology of type 2 diabetes. *Diabetes* 2002;51:7–18.

46. Shimano H, Yahagi N, Amemiya-Kudo M, *et al.* Sterol regulatory element-binding protein-1 as a key transcription factor for nutritional induction of lipogenic enzyme genes. *J Biol Chem* 1999;274:35832–35839.

47. Knebel B, Haas J, Hartwig S, *et al.* Liver-specific expression of transcriptionally active srebp-1c is associated with fatty liver and increased visceral fat mass. *PLoS One* 2012;7:1–15.

48. Reddy JK, Rao MS. Lipid metabolism and liver inflammation. II. Fatty liver disease and fatty acid oxidation. *Am J Physiol Gastrointest Liver Physiol* 2006;290:G852–8.

49. McGarry JD, Leatherman F, Foster W, Am- G. Carnitine palmitoyltransferase I. The site of inhibition of hepatic fatty acid oxidation by malonyl-CoA. *J Biol Chem* 1978;253:4128–4136.

50. Randle PJ. Regulatory interactions between lipids and carbohydrates: The glucose fatty acid cycle after 35 years. *Diabetes Metab Rev* 1998;14:263–283.

51. Sullivan S. Implications of diet on nonalcoholic fatty liver disease. *Curr Opin Gastroenterol* 2010;26:160–164.

52. Bugianesi E, McCullough AJ, Marchesini G. Insulin resistance: A metabolic pathway to chronic liver disease. *Hepatology* 2005;42:987–1000.

53. Oakes ND, Cooney GJ, Camilleri S, Chisholm DJ, Kraegen EW. Mechanisms of liver and muscle insulin resistance induced by chronic high-fat feeding. *Diabetes* 1997;46:1768–1774.

54. Sumiyoshi M, Sakanaka M, Kimura Y. Chronic intake of high-fat and high-sucrose diets differentially affects glucose intolerance in mice. *J Nutr* 2006;136:582–587.

55. Jornayvaz FR, Shulman GI. Diacylglycerol activation of protein kinase Cε and hepatic insulin resistance. *Cell Metab* 2012;15:574–84.

56. Samuel VT, Liu Z, Wang A, *et al.* Inhibition of protein kinase C ε prevents hepatic insulin resistance in nonalcoholic fatty liver disease. *J Clin Invest* 2007;117:739–745.

57. Hernandez TL, Sutherland JP, Wolfe P, *et al.* Lack of suppression of circulating free fatty acids and hypercholesterolemia during weight loss on a high-fat, low-carbohydrate diet. *Am J Clin Nutr* 2010;91:578–585.

58. Choi SM, Tucker DF, Gross DN, *et al.* Insulin regulates adipocyte lipolysis via an Akt-independent signaling pathway. *Mol Cell Biol* 2010;30:5009–5020.

59. Song S, Andrikopoulos S, Filippis C, Thorburn AW, Khan D, Proietto J. Mechanism of fat-induced hepatic gluconeogenesis: effect of metformin. *Am J Physiol Endocrinol Metab* 2001;281:E275–E282.

60. Roden M, Stingl H, Chandramouli V, *et al.* Effects of Free Fatty Acid Elevation on and Gluconeogenesis in Humans. *Endocrinol Metab* 2000:701–707.

61. Clore JN, Glickman PS, Nestler JE, Blackard WG. In vivo evidence for hepatic autoregulation during FFA-stimulated gluconeogenesis in normal humans. *Am J Physiol* 1991;261:E425–E429.

62. Pettinelli P, Obregón AM, Videla LA. Molecular mechanisms of steatosis in nonalcoholic fatty liver disease. *Nutr Hosp* 2011;26:441–450.

63. Fabbrini E, Magkos F, Mohammed BS, *et al.* Intrahepatic fat, not visceral fat, is linked with metabolic complications of obesity. *Proc Natl Acad Sci U S A* 2009;106:15430–15435.

64. Marchesini G, Brizi M, Morselli-labate AM, *et al.* Association of Nonalcoholic Fatty Liver Disease with Insulin Resistance. 9343.

65. Gerber L, Otgonsuren M, Mishra a., *et al.* Non-alcoholic fatty liver disease (NAFLD) is associated with low level of physical activity: A population-based study. *Aliment Pharmacol Ther* 2012;36:772–781.

66. Senn JJ, Klover PJ, Nowak IA, Mooney RA. Interleukin-6 induces cellular insulin resistance in hepatocytes. *Diabetes* 2002;51:3391–3399.

67. Rosen ED, Spiegelman BM. Adipocytes as regulators of energy balance and glucose homeostasis. *Nature* 2006;444:847–853.

68. Tilg H, Moschen AR. Insulin resistance, inflammation, and non-alcoholic fatty liver disease. *Trends Endocrinol Metab* 2008;19:371–379.

69. Hotamisligil GS. Mechanisms of TNF-alpha-induced insulin resistance. *Exp Clin Endocrinol Diabetes* 1999;107:119–125.

70. Korenblat KM, Fabbrini E, Mohammed BS, Klein S. Liver, Muscle, and Adipose Tissue Insulin Action Is Directly Related to Intrahepatic Triglyceride Content in Obese Subjects. *Gastroenterology* 2008;134:1369–1375.

71. Biddinger SB, Hernandez-Ono A, Rask-Madsen C, *et al.* Hepatic Insulin Resistance Is Sufficient to Produce Dyslipidemia and Susceptibility to Atherosclerosis. *Cell Metab* 2008;7:125–134.

72. O'Leary VB, Marchetti CM, Krishnan RK, Stetzer BP, Gonzalez F, Kirwan JP. Exercise-induced reversal of insulin resistance in obese elderly is associated with reduced visceral fat. *J Appl Physiol* 2006;100:1584–1589.

73. Mikus CR, Oberlin DJ, Libla J, Boyle LJ, Thyfault JP. Glycaemic control is improved by 7 days of aerobic exercise training in patients with type 2 diabetes. *Diabetologia* 2012;55:1417–1423.

74. Rabøl R, Petersen KF, Dufour S, Flannery C, Shulman GI. Reversal of muscle insulin resistance with exercise reduces postprandial hepatic de novo lipogenesis in insulin resistant individuals. *Proc Natl Acad Sci U S A* 2011;108:13705–13709.

75. Pescatello L. *ACSM's guidelines for exercise testing and prescription*. Philadelphia: Wolters Kluwer/Lippincott Williams & Wilkins Health; 2014.

76. Donnelly KL, Smith CI, Schwarzenberg SJ, Jessurun J, Boldt MD, Parks EJ. Sources of fatty acids stored in liver and secreted via lipoproteins in patients with nonalcoholic fatty liver disease. *J Clin Invest* 2005;115:1343–1351.

77. Sul HS, Latasa M, Moon Y, Kim K. Symposium : The Role of Long Chain Fatty Acyl-CoAs as Signaling Molecules in Cellular Metabolism Regulation of the Fatty Acid Synthase Promoter by Insulin 1 , 2. 2000:315–320.

78. Shimomura I, Matsuda M, Hammer RE, Bashmakov Y, Brown MS, Goldstein JL. Decreased IRS-2 and increased SREBP-1c lead to mixed insulin resistance and sensitivity in livers of lipodystrophic and ob/ob mice. *Mol Cell* 2000;6:77–86.

79. Calles-Escandón J, Goran MI, O'Connell M, Nair KS, Danforth E. *Exercise increases fat oxidation at rest unrelated to changes in energy balance or lipolysis.* 1996.

80. Poehlman ET, Gardner AW, Arciero PJ, Goran MI, Calles-Escandon J. Effects of endurance training on total fat oxidation in elderly persons. *J Appl Physiol* 1994;76:2281–2287.

81. Tunstall RJ, Mehan KA, Wadley GD, *et al. Exercise training increases lipid metabolism gene expression in human skeletal muscle.* 2002.

82. Trajcevski KE, O'Neill HM, Wang DC, *et al.* Enhanced Lipid Oxidation and Maintenance of Muscle Insulin Sensitivity Despite Glucose Intolerance in a Diet-Induced Obesity Mouse Model. *PLoS One* 2013;8.

83. Bielohuby M, Sisley S, Sandoval D, *et al.* Impaired glucose tolerance in rats fed low-carbohydrate, high-fat diets. *Am J Physiol Endocrinol Metab* 2013;305:E1059–70.

10. Appendices

10.1 Appendix A - Detailed Experimental Methods

10.1.1 Lysis Buffer for Homogenization

Reagent	Concentration/MW
NaCl	135mmol/L (MW=58.44)
$MgCl_2$	1mmol/L (MW=203.3)
KCl	2.7mmol/L (MW=74.55)
Tris (pH 8)	20mmol/L (MW=121.14)
Triton 1%	
Glycerol 10%	

Prepare lysis buffer stock and store at -20°C. Aliquot desired volumes and add protease (cOmplete ULTRA Tablets) and phosphatase (PhoStop) inhibitors immediately prior to use.

Laemmli Sample Buffer (2x) - (Bio-Rad, Cat#161-0737)
Per 1mL: 950µl of 2x Laemmli sample buffer
50Ul β-Mercaptoethanol

Store at room temperature. Dilute the sample (1 in 2) with sample buffer and heat for 5min at 95°C.

10.1.2 Preparation of Tissue Lysates

1. Upon extraction, immediately snap freeze samples and store at -80°C.
2. Weigh sample (~ 20mg for liver) and add to 350µl of lysis buffer containing both protease & phosphatase inhibitors. (Always keep samples on ice and avoid thawing while weighing tissue)
3. Thoroughly homogenize the sample.
4. Centrifuge the tissue lysate for 10min @ 12,000rpm (4°C).
5. Extract the supernatant and transfer to a fresh micro tube.
6. Take one aliquot for protein determination by Bradford method.
7. Aliquot remaining lysate and store at -80°C.
8. For western blot purposes, dilute lysates with 2x lammeli buffer (1 to 1 v/v) as needed and heat for 5 min at 95°C prior to use.

10.1.3 Western Blotting Buffers

10x Electrophoresis/Running Buffer (pH - 8.3)
30.34g Tris base
144g Glycine
10g SDS
Dissolve contents in 1L of ddH_20 and store at room temperature.

1x Running Buffer (pH- 8.3)
10% 10x Running buffer
90% ddH_20
Mix solutions and store at room temperature.

10x Transfer Buffer (pH- 8.3)
30.3g Tris base
144g Glycine
Dissolve contents in 1L of ddH_20 and store at room temperature.

1x Transfer Buffer (pH- 8.3)
10% 10x Transfer buffer
20% Methanol
70% ddH_20
Mix solutions and store at -20°C prior to use.

10x Wash Buffer
60.57g Tris base
87.66g Sodium Chloride (NaCl)
Dissolve contents in 1L of ddH_20, store at room temperature.

1x Wash Buffer
10% 10x Wash buffer
90% ddH_20
Add 500Ul/L of Tween-20 and NP-40. Mix solutions and store at room temperature.

Blocking Buffer
3% BSA (w/v: 1.5g/50mL)
Dissolve in 1x Wash buffer, store at 4°C.

Antibody (Ab) Buffer
1° Ab – 1 part blocking buffer + 2 parts wash buffer + 0.02% NaAzide (stock in ddH_20)
2°Ab – 1 part blocking buffer + 2 parts wash buffer (NO NaAzide).
Typically 1:1000-1:2000 dilution is appropriate for an Ab. This may vary depending on how good the signal is.

Resolving gl Tris Buffer (1.5M) (pH-8.8)
90.86g/500mL of ddH_20

Stacking gel Tris Buffer (0.5M) (pH-6.8)
30.3g/500mL of ddH_20

10% APS Solution
10% (w/v) Ammoniumperoxide Sulfate in ddH_20.
Use 0.1g/mL
Store at -20°C.

10% SDS Solution
10% (w/v) Sodium dodecylsulfate in ddH_20
Use 1g/10mL
Store at room temperature.

10.1.4 Western Blotting

1. Take samples out of -80° freezer and place on ice.
2. Place gels into cassettes, and add the cassette to tank ensuring red and black terminals of cassette correspond with red and black markings of tank respectively.
3. Add 1x running buffer to fill the tank.
4. Once samples have thawed, spin in centrifuge for a few seconds.
5. Take out combs from gel and pipette 7ul Bio-Rad protein ladder.
6. Add samples into each well according to Bradford values.
7. Top up with running buffer to make sure tank is full.
8. Ensure positive and negative electrodes are matched (black to black, red to red)
9. Turn on the voltage for 60V for 30min, and then turn it up to 110V for ~1.5hrs until dye runs off the gel.
10. While gel is running, can prepare 1x transfer buffer. Once transfer buffer is well mixed, cover with parafilm and place in the -20°C freezer until ready for transfer.

Transferring the Gel onto a membrane

1. Fill Pyrex dish with cold transfer buffer.
2. Cut out equal sized membranes and dip in methanol to activate (2min). Also cut out equal sized filter papers and prepare the appropriate number of foam pads.
3. Place membranes in transfer buffer after activation.
4. Once dye has run off the gel, remove the gels from tank and soak in transfer buffer. Carefully remove glass plates. Cut off and discard combs of the gel. Loosen gel from the glass plate with scraper while keeping it emerged in the buffer.
5. In the pyrex dish, place the black side of the cassette on the bottom, and place two foam pads followed by 3 filter papers on top. Ensure there are no bubbles.
6. Carefully place gel on top of filter paper and use the roller to get any air bubbles out. Make sure gel is in the correct orientation so that the ladder will appear on the left side of the membrane when removed.
   Note: transfer runs from negative (black) to positive (red). Always ensure proteins will run from gel to the membrane.
7. Carefully place the membrane on top of the gel and roll out any bubbles.
8. Place 3 more filter papers on top and roll out any bubbles.
9. Add one foam pad and roll out any bubbles.
10. Carefully close sandwich and place into transfer tank. Make sure black matches black and red matches red.
11. Place ice pack in tank to keep buffer cold. Close the lid ensuring positive and negative electrodes are matched (black to black, red to red)

11. Surround transfer tank with ice to keep cold.
12. Turn on transfer at 120V for 2.5 hours or at 60V overnight.
13. Look for bubbles on ends of cassette to indicate successful transferring.
14. Check on temperature throughout transfer time to ensure no overheating.

Probing the membrane

1. Prepare containers to hold blocking buffer for each membrane, approx. 10mL per container.
2. Once transfer has finished, open cassettes and quickly place membranes in containers with blocking buffer.
3. Allow the membranes to surf in the blocking buffer for 1hr at room temperature on the orbital shaker.
4. Pour out blocking buffer and add 1°Ab.
5. Incubate overnight on shaker at 4°C. Ensure containers are fully sealed to avoid evaporation.
6. The next day, remove 1°Ab and wash membranes 5x at 10min intervals with 10mL of 1x wash buffer to rid the membrane of any unbound Ab.
7. Add 2° Ab and allow membranes to surf on orbital shaker for 1hr at room temperature.
8. Remove 2°Ab and wash membranes 5x at 10min intervals with 10mL of 1x wash buffer to rid the membrane of any unbound 2°Ab.
9. Membranes are ready for developing

Developing the membrane

1. For each membrane, use 3mL chemiluminescence (Millipore Immobilon Western Chemiluminescent HRP substrate) per membrane and incubate for 3 minutes.
2. Dip membranes into ddH_20 to rinse and place in radiography cassette.
3. In the darkroom, expose film for desired time.
4. Place film in developer for a few seconds until signal appears. Dip into water to stop the reaction, and place in fixer solution. Ensure ample fixing time.
5. Rinse with water and allow drying.

10.1.5 Buffers for liver slice incubation

Stock solutions for Krebs Ringer Bicarbonate (KRB) Buffer
Note: All solutions are made with ddH_2O

Quantity	Reagent/Molarity
0.9g in 100ml	0.154M NaCl (mw = 58.44)
575mg in 50ml	0.154M KCl (mw = 74.55
610mg in 50ml	0.11 $CaCl_2$ (mw = 110.99)
1.055g in 50ml	0.154M KH_2PO_4 (mw = 136.09)
927mg in 50ml	0.154M $MgSO_4$ (mw = 120.30)
650mg in 50ml	0.154M $NaHCO_3$ (mw = 84.01)

*Gasify $NaHCO_3$ with carbogen (95% O_2/5% CO_2) for 1h after assembly. Stock solutions can be stored at 0-4°C.

KRB Buffer Assembly (for 100ml)
Note: Adjust volumes accordingly depending on number of samples.

For 100ml of KRB buffer:

Quantity	Reagent/Molarity
78.6ml	0.154M NaCl
3.08ml	0.154M KCl
2.32ml	0.11 $CaCl_2$
0.768ml	0.154M KH_2PO_4
0.768ml	0.154M $MgSO_4$
16.1ml	0.154M $NaHCO_3$
100mg	5.5mM Glucose
715mg	30mM Hepes

Once assembled, the KRB solution is gasified for 45min with carbogen (95% O_2/5% CO_2). pH the gasified KRB buffer to 7.4 using 10N NaOH. Finally add fatty acid free BSA (Sigma Cat# A3803) to the solution at a concentration of 4% (40mg/ml).

For glycogen synthesis and glycogen content assays, take the required amount of KRB Buffer and add radiolabelled D-[^{14}C] glucose at a concentration of 0.2 μCi/ml.

10.1.6 Incubation of liver slices for Glycogen Synthesis & Glycogen Content

1. Warm up the water bath to 37°C
2. Fill pre-incubation scintillation vials with 2ml of KRB-BSA buffer & place in the water bath.
3. Fill basal scintillation vials with 2ml of KRB-BSA containing 0.2 μCi/ml D-[^{14}C] glucose.
4. Add insulin (100nM) to the remaining KRB-BSA containing D-[^{14}C]glucose.
5. Add this insulin/radiolabelled-glucose containing KRB buffer to the insulin-stimulation scintillation vials.
6. Ensure that all vials are capped with rubber stoppers and continuously gasified with carbogen (95% O_2/5% CO_2) at a steady rate.
7. Extract a slice of liver weighing ~ 20mg (along the edges of the organ) being careful not to inflict damage to the tissue. Keep it moist at all times with ice-cold PBS.
8. Gently place the slice into the scintillation vial. *All slices are in pre-incubated for 1h. Subsequently, the slice is transferred to a second vial (basal or insulin-stimulated in the presence of D-[^{14}C] glucose) and incubated for another hour.
9. At the end of the second hour, remove the slice from the vial and immediately dip in liquid nitrogen to freeze the reaction.
10. Place the frozen slice in 500ul of 1N KOH for digestion for 30min @ 90°C.
11. Keep 100ul for glycogen content (-80°C) and 400ul for glycogen synthesis assays (-20°C).

10.1.7 Glycogen Content Reagents

Note: Adjust volumes accordingly depending on number of samples.

Acetate Buffer (0.2M, pH 4.8)
480µl Acetic Acid (98%)
975mg Sodium Acetate
Complete to 100ml using ddH_20. Adjust pH to 4.8 and store at 0-4°C.

Amyloglucosidase Solution
1mg Amyloglucosidase Enzyme Protein Powder
1ml 0.2M Acetate Buffer

1N KOH (pH off the scale)
5.61g KOH
Complete to 100ml using ddH_2O.

Triethanolamine (TRA) Buffer (0.3M TRA; 4.05mM $MgSO_4$; 1N KOH, pH 7.5)

5.6g Triethanolamine
100mg $MgSO_4$
12ml 1N KOH
Complete to 100ml using ddH_2O. Store at 0-4°C

Ammonium Sulfate (3.2M)
4.23g $(NH_4)_2SO_4$
Complete to 10ml with ddH_2O.

Hexokinase/G6PDH Suspension
500U (based on HK units – 125U/mg of protein. There is ~ 4mg of protein per vial.
Re-suspend the lyophilized enzyme in 2ml of 3.2M Ammonium Sulfate (~ 250U/ml).

ATP-TRA Buffer (1mM ATP; 0.9mM NADP; 5ug/ml HK/G6PDH)
6mg ATP
8mg NADP
10ml TRA Buffer
50µl HK/G6PDH Suspension
Note: Solution is stable for one week at 0-4°C.

10.1.8 Glycogen Content

1. Transport the liver slice (weighing ~ 20-30mg) to a 1.5ml eppendorf and add 500µl of 1M KOH.
2. Incubate the sample on the heat block for 30min @ 90°C.
3. 15min into the incubation period gently shake the eppendorf around once to ensure complete digestion.
4. Extract 100µl for glycogen content and place in an eppendorf. The remaining 400µl may be used for a glycogen synthesis assay if desired.
5. Add 10% (v/v) of acetic acid 17.5M to digested tissue (maintains pH between 4-5, ideally 4.8 which is optimum for hydrolysis of glycogen by amyloglucosidase).
6. Add 500µl of acetate buffer (4.8 pH) with amyloglucosidase (0.5mg/ml).
7. Incubate for 2h at 40°C with shaking or on bench overnight.
8. Neutralize the solution with 1/16 (v/v) of NaOH (5N). pH should now be 7.37 @ 25°C.
9. Centrifuge for 5min @ 3000rpm.
10. Extract 400µl of the digested supernatant & add 1ml of ATP-TRA Buffer.
11. Incubate for 30min on the bench.
12. Gently vortex and extract 1ml and dispense into a plastic cuvette.
13. Read the OD at 340nm. Note: (OD x 8.89) = umol of glucosyl units.
14. Correct readings for tissue weight.

10.1.9 Glycogen Synthesis Reagents

Note: Adjust volumes accordingly depending on number of samples.

1N KOH (pH off the scale)
5.61g KOH
Complete to 100ml using ddH2O

Saturated Na_2SO_4
Dissolve powdered Na_2So_4 in ddH_2O until precipitation forms. Precipitate formation is a sign of saturation.

Cold Ethanol
Place 100% Ethanol in a 50ml falcon tube. Leave in -20°C.

10.1.10 Glycogen Synthesis (Incorporation of D-[14C] glucose into Glycogen)

1. Transport the liver slice (weighing ~ 20-30mg) to a 1.5ml eppendorf and add 500µl of 1M KOH.
2. Incubate the sample on the heat block for 30min @ 90°C.
3. 15min into the incubation period gently shake the eppendorf around once to ensure complete digestion.
4. Extract 400µl for glycogen content and place in a 2ml eppendorf.
5. Add 100µl of carrier glycogen to each sample.
6. Add 80µl of saturated Na_2SO_4 to each sample
7. Add 1.2ml of cold ethanol
8. Gently vortex each sample and incubate at -20°C overnight to allow precipitation.
9. On the following day, check for precipitation and centrifuge the samples for 20min @ 3000rpm.
10. Discard the resultant supernatant.
11. Dissolve the pellet in 500µl of ddH_20.
12. Extract 400µl of sample and add to 5ml of scintillation fluid (ECOLITE+ liquid scintillation cocktail (MP Biomedicals Cat #01882475)) for counting.

10.1.11 Measuring Glucose 6-Phosphate using commercially available Calorimetric Kit

Abcam, Cat # ab83426

Sample Preparation (Ensure samples are always on ice throughout procedure)

1. Weigh out 50mg of liver and homogenize in 2-3 volumes of ice cold PBS.
2. Centrifuge the sample for 10min @ 12,000rpm (4°C).
3. Extract the supernatant and place into a 10kDa molecular weight cut-off spin column (cat#UFC501008).
4. Centrifuge the spin column for 1h @ 12,000rpm (4°C).
5. Extract the lysate collected at the bottom of the column and dispense in a separate eppendorf. Keep on ice.

Reaction mix Preparation

Note: Prepare enough for the number of samples and standards you plan on running.

	Reaction Mix	**Background**
Assay Buffer	46µl	48µl
Enzyme Mix	2µl	---
Substrate Mix	2µl	2µl

Prepare Standard Curve & Run Samples

1. Dilute the stock G6P standard (100nmol/ µl) to 1nmol/µl by adding 10µl of the stock to 990µl of ddH_2O
2. Add the diluted standard to a 96-well plate by pipetting 0,2,4,6,8,10µl into a series of wells.
3. Add 1-50µl of sample to the wells.
4. Use assay buffer to adjust volume of both samples and standards to 50µl/well.
5. Add 50µl of reaction mix to standards (excluding the 0) and samples.
6. Add 50ul of background mix into the 0 standard (background).
7. Incubate on the bench for 30min. Protect from light.
8. Use the plate reader to measure at 450nm.
9. Subtract the background from all standards and samples.
10. Concentration = Ay/Sv, where Ay is the amount of G6P (nmol) in your sample and Sv is the volume (µl) of sample added to the well.

10.1.12 Complexation of Palmitic Acid

1. Prepare 30mL of KRB Buffer (without glucose)
2. Add 3.75g FA-free BSA (Sigma Cat# A3803) to get a 12.5% solution
3. Heat to 50°C in water bath
4. Take 1600mg palmitic acid (Sigma Cat# P-5585) to put into a 2mL eppendorf
5. Dissolve palmitic acid with 100µl NaOH (10N) and vortex vigorously
6. Add palmitic acid into preheated medium while stirring. (note; it will precipitate)
7. Pour into falcon tube, protected from light
8. Incubate in 50°C water bath for 4+ hours while shaking at 150-200rpm
9. After the incubation period, filter solution to get chunks out using a 10mL syringe and sterile strainer
10. pH to 7.4
11. Aliquot solution and store at -20°C

10.1.13 Determination of FFA using Wako Pure Chemicals HR Series NEFA –HR Kit

1. Dissolve Reagent A into Solvent A
    - 4.1mg of Reagent A per 1mL of solvent A (calculate total volume you need for samples and standards)
2. Add 0.5mL of Reagent A solution into each cuvette and incubate for 5 min at 37°C
3. Dissolve Reagent B into Solvent B
    - 10.6mg of Reagent B per 1mL of solvent B
4. Add 0.25mL of Reagent B solution into each cuvette and incubate for 5 min at 37°C
5. Read at OD 550nm

Cuvette	1mEq/L NEFA Std (µL)	H_20 (µL)	Reagent A Sol. (mL)	INCUBATE	Reagent B Sol. (mL)	INCUBATE	Optical Density 550nm	NEFA Conc. (mEq/L)
Blank	-	12.5	0.5		0.25		0 (Ref)	0
0	-	12.5	0.5		0.25		0	0
Low Std	6.25	6.25	0.5		0.25		read	0.5
Mid Std	12.5	-	0.5		0.25		read	1.0
High Std	25	-	0.5		0.25		read	1.97
Sample	12.5	-	0.5		0.25		read	TBD

10.1.14 Incorporation of [1-14C] Palmitic acid into 14CO2 (Palmitate Oxidation)

1. Warm up the water bath to 37°C
2. Add 200mM of complexed palmitate and 0.2µCi/ml [1-^{14}C] Palmitic acid to KRB buffer.
3. Add 2ml of this buffer to the scintillation vial and incubate.
4. Ensure that all vials are capped with rubber stoppers and continuously gasified with carbogen (95% O_2/5% CO_2) at a steady rate.
5. Obtain a slice of liver weighing ~ 20mg (along the edges of the organ) being careful not to inflict damage to the tissue. Keep it moist at all times with ice-cold PBS.
6. Place the slice in the KRB-BSA medium containing [1-^{14}C] palmitate
7. Gasify using carbogen for 1 hour.
8. After 1 hour, add 200µl (1:1, vol/vol) 2-phenylethylamine/methanol into a vial containing filter paper.
9. Gently place this vial into the scintillation vial containing the sample. Reapply the rubber stopper and incubate for another hour with gasification using carbogen.
10. Carefully, use a syringe to add 200µl of H_2SO_4 (5N) to the incubation medium making sure not to add any to the 2-phenylethylamine/methanol containing vial. The cap must remained closed while adding H_2SO_4 (5N). Incubate for 1h without gasification.
11. Remove filter paper and place in a scintillation vial containing 10ml of scintillation fluid (ECOLITE+ liquid scintillation cocktail (MP Biomedicals Cat #01882475))

10.1.15 Measuring Triglyceride Content using commercially available Calorimetric Kit

Note: This procedure can be done over one or two days.

Materials

- Triglyceride Quantification Kit (100 samples including 6 standards) (Cat# ab65336)
- 5ml Tubes (1 tube/sample)
- 5% NP40
- ddH_2O

Day 1 – Sample Preparation

1. Determine the number of samples to be assayed and make an appropriate amount of 5% NP40 (diluted in water) (1ml/sample).
2. Add 100mg of tissue (liver) to 1ml of 5% NP40 in a 5ml tube.
3. Heat the sample in the water bath for 10min @ 90°C.
4. Homogenize the sample in the 5ml tubes.
5. Heat the homogenized sample for 5min @ 90°C.
6. Remove the tubes from the water bath and let them cool down to room temperature.
7. Heat the sample once again for 5min @ 90°C.
8. Centrifuge the samples for 2 min at max speed.
9. Extract 20 µl for measuring protein content and store in an eppendorf.
10. Extract the remaining sample from the 5ml tubes and dispense into a separate eppendorf. (Be sure not to extract any insoluble material)
11. Store the samples at -80°C or continue procedure.

Day 2 – Prepare Standard Curve and Run Samples.
Note: Be sure to make room for 1 blank/condition.

1. Allow samples to thaw.
2. Vortex the samples and centrifuge them @13,200rpm for 10min.
3. While vortexing, reconstitute the enzyme mix in 220µl of assay buffer. Also, reconstitute the lipase in 220µl of assay buffer. Make aliquots and store unused portion in -20°C.
4. Dilute the stock standard (1mM) to 0.2mM by adding 100µl of the stock to 400µl of assay buffer provided in the kit.
5. Take a 96-well plate and start putting in the standards. Add 0µl, 10µl, 20µl, 30µl, 40 µl, and 50 µl of the 0.2mM standard in series.
6. Use assay buffer to top up all standards to a final volume of 50µl.
7. Dilute each of sample 10x by adding 10µl of sample to 90µl of ddH_2O. Mix well.
8. For liver put 25 µl of the diluted sample per well. Top sample wells off to 50µl/well by adding 25µl of assay buffer.

9. Add 2ul of lipase to every well INCLUDING the standards. For blanks (1 blank/condition) add 2µl of assay buffer instead of the lipase. (This is the only difference between blanks and samples)
10. Let the well incubate for 20 min (Gently shake for 2min. Use the remaining 18min to make reaction mix).
11. Reaction mix (Light sensitive. Wrap in foil immediately. Store at room temperature)

	Reaction Mix
Assay Buffer	46µl
Triglyceride Probe	2µl
Enzyme Mix	2µl

12. Add 50µl of reaction mix to ALL wells including standards and blanks.
13. Shake the plate for 2min and incubate in a light-protected area for 1h.
14. Use the plate reader to read at 570nm.
15. Subtract your blanks from your samples.
16. Subtract absorbance of blank (standard 0) from all standards and samples.
17. Calculate concentration.

10.1.16 Measuring Circulating Insulin by ELISA

1. Fast the animals for 14-hr then obtain a blood sample from the saphenous vein.
2. Always keep blood on ice.
3. Centrifuge the blood at for 10min @ 13,000rpm (4°C)
4. Extract the plasma (supernatant) and place into another labeled eppendorf. Store at -80°C until you are ready to run the ELISA.
5. When ready to assay, pre-warm all reagents of the EMD Millipore ELISA kit (Cat. # EZRMI-13K) to room temperature.
6. Dilute the provided 10X wash buffer by 10-fold.
7. Determine the number of samples to be assayed and place any extra microtiter strips in 2-8°C.
8. Place the microtiter strips that you will be using in a plate holder and wash 3 times with 300µl of diluted wash buffer.
9. Remove buffer from wells by tapping lightly onto an absorbent surface DO NOT let the wells dry completely.
10. Add 10µl of assay buffer to each blank & sample wells.
11. Add 10µl of Matrix solution to blank, standard, and control wells.
12. Add 10µl of 0.2, 0.5, 1, 2, 5 and 10 ng/mL insulin standards in ascending order.
13. Add 10µl of quality control 1 & 2 into their own wells.
14. Add 10µl of sample into the remaining wells.
15. Add 80ul of detection antibody to all wells
16. Seal the plate and incubate at room temperature for 2h on an orbital shaker
17. Remove plate sealer and tap onto an absorbent surface to empty contents.

18. Wash the plate 3 times with 300µl of wash buffer by decanting after each wash.
19. Add 100 µl of enzyme solution to each well. Seal with plate sealer and incubate for 30min at moderate speed on an orbital shaker.
20. Remove the seal and decant the contents.
21. Wash 6 times using diluted wash buffer making sure to decant contents after each wash.
22. Add 100 µl of substrate solution to each well. Cover with plate sealer and shake for 20 min on orbital shaker.
23. Add 100µl of stop solution to each well and mix well by hand. Ensure there are no bubbles and read using a plate reader at 450 and 590nm. Record absorbance.
24. Calculate insulin concentrations as outlined in the manual.

10.2 Appendix B - Statement of Labor

All experiments conducted in this study were carried out by Abinas Uthayakumar (AU), Diane Sepa-Kishi (DSK), Michelle Victoria Wu (MVW) and Arta Mohasas (AM). All were involved in the training of animals, collection of food intake and body weight data, extraction of tissues, IPGTT, IPPTT, and measuring palmitate oxidation. AU was responsible for measuring glycogen synthesis, glycogen content, and G6P with the help of AM. Moreover, AU conducted the western blots presented in this study. Due to the logistics of this experiment, AM quantified liver triglycerides, while DSK and MVW conducted experiments for lipolysis.

Dr. Rolando Ceddia is the primary investigator and supervisor of this project and this research was funded by the Natural Sciences and Engineering Research Council of Canada (NSERC) grant 311818-2011.